universität wien

DIPLOMARBEIT

Titel der Diplomarbeit

Modelling Heavy Ion Fusion Reactions Using the Proximity Potential

verfasst von

Manuela Gober, Bakk. rer. nat.

angestrebter akademischer Grad

Magistra der Naturwissenschaften (Mag. rer. nat.)

Wien, 2013

Studienkennzahl lt. Studienblatt:	A 411
Studienrichtung lt. Studienblatt:	Physik
Betreut von:	Ao. Univ.-Prof. Mag. Dr. Harry Friedmann

Abstract

The aim of this diploma thesis is to make a contribution to modelling heavy ion fusion reactions in the range of the coulomb barrier height. The nucleus-nucleus interaction potential consists of the coulomb potential and the nuclear potential. In this thesis the nuclear potential is calculated by using the proximity potential [1]. For this task already well known nuclear properties, such as surface energy coefficient, rms nuclear charge radii, etc., are used. Because of that, no adaptation of experimentally measured data or measurements need to be undertaken.

By applying additional aspects on the calculation of the nucleus-nucleus interaction potential by neck formation [2] and extra push [3], corrected barrier heights are gained. These new barrier heights are used to estimate the fusion cross section by using the distributed barrier model [4] for each reaction.

A comparison between the results of Siwek-Wilczyńska et al. [4] using the woods-saxon potential in conjunction with the distributed barrier potential, which states that no acceptable results are gained by the proximity potential, shows that the modification of the proximity potential by inclusion of neck formation and extra push produces almost as good as results as the woods-saxon potential [4] with fitted parameters.

In this work one gets by using this modified model of the proximity model the barrier height and its location radius for all reactions, which are used in the distributed barrier function [4] in order to receive the excitation function.

For the analysis 48 fusion reactions [4] were examined and compared to results of other models. The calculation was executed in the scientific program MATLAB R2008b and is attached in the appendix.

Abstract

Das Ziel dieser Diplomarbeit ist es, in der Modellierung von Schwerionenreaktionen im Bereich der Coulomb-Barriere einen Beitrag zu leisten. In dieser Arbeit wird zur Berechnung des nuklearen Potentials, welches neben dem Coulomb-Potential in das wechselwirkende Potential zwischen den Atomkernen miteinfließt, das Proximity-Potential herangezogen [1]. Dafür werden wohl bekannte nukleare Größen wie der Oberflächenenergie-Koeffizient, rms Ladungsradien, etc. verwendet. Aufgrund dessen ist eine Anpassung an experimentellen Werten nicht von Nöten.
Durch die Anwendung weiterer Aspekte wie Neck Formation [2] und Extra Push [3] in der Berechnung des wechselwirkenden Potentials, werden korrigierte Werte der Barrierenhöhen erhalten. Diese neuen Barrierenhöhen werden verwendet, um eine Abschätzung der Fusionswirkungsquerschnitte mittels dem "distributed barrier model" [4] für jede Reaktion zu ermöglichen.
Ein Vergleich mit den Ergebnissen unter der Verwendung des Woods-Saxon Potential mittels dem "distributed barrier model" von Siwek-Wilczyńska et al. [4], nach welchen das Proximity-Potential keine akzeptablen Werte ergibt, zeigt aber, dass die Modifikation des Proximity-Potentials durch Einbeziehen der Neck Formation und des Extra Push fast so gute Werte liefert wie das Woods-Saxon-Potential [4] mit angepassten Werten.
In dieser Arbeit wird dieses modifizierte Proximity-Potential herangezogen um die Barrierenhöhen sowie deren Position zu berechnen. Diese fließen in die Distributed Barrier Function [4] ein, welche die Anregungsfunktion einer Reaktion liefert.
Für die Analyse wurden 48 Fusionsreaktionen [4] betrachtet und ein Vergleich zu den Ergebnissen von anderen Modellen wurde angestellt. Die Berechnung wurde mittels des wissenschaftlichen Programms MATLAB R2008b durchgeführt und ist im Anhang beigelegt.

Contents

1 Introduction

1.1 Motivation

The nucleus-nucleus interaction potential of two fusing nuclei needs to be studied, as it is a mathematical challenge in determining the nuclear part of the interacting potential via coupled channel calculations. Different kinds of nucleus-nucleus interacting potential have been introduced in the last decades. By using the proximity potential for the calculation of the nuclear part, one can get an acceptable theoretical value for the barrier height and its location in comparison to the experimentally measured values. With this easy to handle calculation tool for which no fitting to experimental data is needed, one can approximately estimate fusion cross section for any heavy ion fusion reaction without any measurements. This possibility of prediction about characteristics of fusion reactions (such as barrier height, fusion cross section, etc.) is significant for research, especially for the formation of superheavy elements by nucleosynthesis.

1.2 State of Research

Different investigations into the prediction of barrier height and the location of radius of fusion reactions have been made. These investigations differ in various kinds of nuclear potentials (such as the proximity potential or the woods-saxon potential) for fusion reactions, in different modifications of the potentials or in varying the parameters of a potential itself.

The original form of the proximity potential [5] was used by Vaz et al. [6] for calculation of barrier heights and their location radius for 96 measured fusion barriers at low energies. This model features a 4% deviation on average to the experimentally measured values [1]. Further modifications of the original proximity potential model improved this overestimation.

Myers et al. [1] used a modified form of the proximity potential for the calculation by using up-to-date values of nuclear parameters (e. g. surface energy coefficient and nuclear radius). For the analysis, they studied the same data as Vaz et al. (96 measured fusion barriers at low energies) [6]. The results showed an average deviation for all 96 fusion reactions of about -0.01% and the rms spread of the deviation was 3.30%.

Another modified proximity potential model has been analysed by Dutt [7]. In this model a new formula for the nuclear charge radius has been used. Furthermore, the surface energy coefficient was taken from [8]. For their analysis, they viewed 395 fusion reactions at low and intermediate energies. The mean deviation in the determined barrier height values by this modified proximity potential model is about 0.30 MeV to the experimental values.

Siwek-Wilczyńska et al. [4] analysed the fusion excitation functions at low energies of 48 measured reactions and determined by using the distributed barrier function the barrier heights of each fusion

reactions. This model reproduces theoretical barrier heights to within a deviation of less than 1 MeV in mean to the experimental values.

An advantage of the modified model used in this work is that no fitting of parameters to experimental data will be needed, whereas all models named above need fitted parameters.

1.3 Level of Ambition

Here the author wants to modify the proximity potential by including different kinds of corrections, so that the predicted results of the modified nucleus-nucleus interaction potential represent acceptable values of the barrier height of a fusion reaction and the position of the barrier-maximum without fittings to experimental data. To improve the original results [6], neck formation is taken into account for the calculation of the barrier height. The theory of the extra push is also included.
This model is still a simplified model as deformation of the participating nuclei and other phenomena (quantum effects, etc.) are disregarded. But in spite of these simplifications, this model produces good results as can be seen in the analysis chapter.
The gained results for the position and height of the barrier are used in the distributed barrier model [4] and results in acceptable accuracy at about the same level as the latest models feature but with the additional advantage no fitting to experimentally measured data is needed.

2 Fusion

Fusion describes the process of conflation between two colliding nuclei and occurs in all mass ranges. For this task, the participating nuclei need to overcome the fusion barrier, which is determined by the potential of the repulsive coulomb force and the attractive nuclear force [9].
Fusion of light particles is the process responsible for the production of energy in stars. Elements up to iron are formed by stellar nucleosynthesis. Elements of a higher proton number than iron ($Z = 26$) are formed either by the r- and/or s-processes. Uranium is the last element which is formed naturally and still exist on earth. All elements with a higher proton number than uranium ($Z = 92$) are formed synthetically. These are produced by heavy ion fusion reactions. Niels Bohr presented the hypotheses of compound nuclear reactions [9] in which an intermediate nucleus in the fusion process is introduced. In this case projectile a and target A fuse to an extremely excited compound nucleus C^*, which decays into an ejectile b and a final nucleus B [9]:

$$a + A \longrightarrow C^* \longrightarrow b + B \tag{2.1}$$

It is assumed that entry channel and exit channel are independent of each other. The fusion process in the entry channel can occur for all kinds of compositions of nuclei [9].
As for other nuclear reactions there are conservation laws for the fusion process:

- Conservation of the charge q

$$q_a + q_A = q_b + q_B \tag{2.2}$$

- Conservation of the energy E

$$E_a + E_A + m_a c^2 + m_A c^2 = E_b + E_B + m_b c^2 + m_B c^2 \tag{2.3}$$

- Conservation of linear momentum $\overrightarrow{p}$

$$\overrightarrow{p}_a + \overrightarrow{p}_A = \overrightarrow{p}_b + \overrightarrow{p}_B \tag{2.4}$$

- Conservation of the total angular momentum $\overrightarrow{J}$

$$\overrightarrow{J}_{a,A} = \overrightarrow{s}_a + \overrightarrow{s}_A + \overrightarrow{l}_{a,A} = \overrightarrow{s}_b + \overrightarrow{s}_B + \overrightarrow{l}_{b,B} = \overrightarrow{J}_{b,B} \tag{2.5}$$

  with the total angular momentum $\overrightarrow{J}$ as the sum of the spin $\overrightarrow{s}$ of each particle and the orbital angular momentum of the relative movement $\overrightarrow{l}$.

- Conservation of the parity π

$$\pi_a \cdot \pi_A \cdot (-1)^{l_{a,A}} = \pi_b \cdot \pi_B \cdot (-1)^{l_{b,B}} \tag{2.6}$$

- Conservation of the isospin $\overrightarrow{T}$

$$\overrightarrow{T_a} + \overrightarrow{T_A} = \overrightarrow{T_b} + \overrightarrow{T_B} \tag{2.7}$$

- Conservation of the baryon number

$$A_a + A_A = A_b + A_B \tag{2.8}$$

with the mass number A.

3 Nucleus-Nucleus Interaction Potential

The nucleus-nucleus interaction potential for two approaching nuclei can be written as [1]

$$V(r) = \frac{Z_1 Z_2 e^2}{r} + V_{nuc} \qquad \text{for} \quad s > 0 \tag{3.1}$$

Here Z_1 and Z_2 are the proton numbers of each nucleus, r describes the center separation radius of the two colliding nuclei and e is the charge unit.

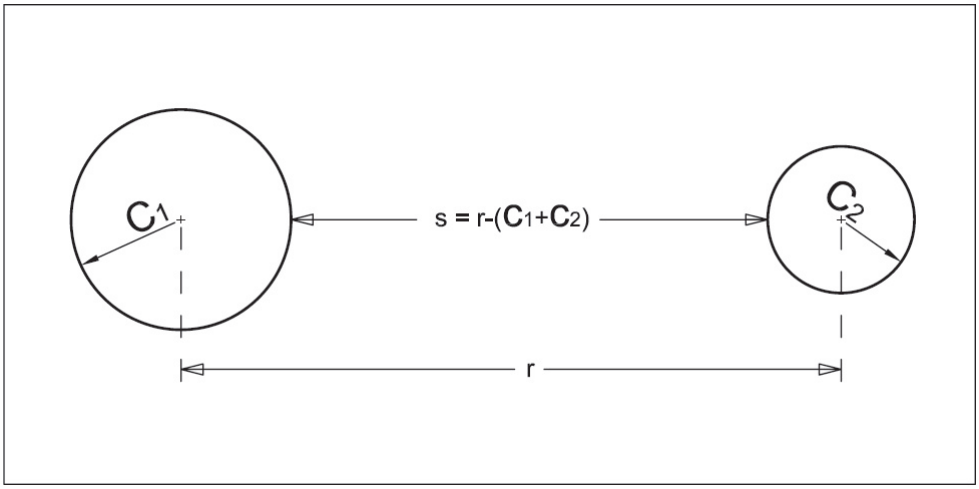

Figure 3.1: Illustration of two approaching nuclei with matter radius C_1 and C_1 at a center separation distance r

The first term of equation (3.1) describes the coulomb potential which is well known and has a long range and a repulsive character against fusion processes. It is defined only for positive values of the contact separation s, as the electrostatic repulsion is defined for this range [7]. The second term is the nuclear potential in the form of the proximity potential which is based on the short-range and attractive nuclear force.

3.1 Proximity Potential

The proximity potential is based on the proximity force theorem [5] which says that "the force between two gently curved objects in close proximity is proportional to the interaction potential per unit area between two flat surfaces made of the same material, the constant of proportionality being a measure of the mean curvature of two objects. This theorem leads to a formula for the interaction potential between curved objects (e. g. two atomic nuclei) which is a product of a simple geometrical factor and a universal function of separation, characteristic of the material of which the objects are made, and intimately related to the surface energy coefficient".

In following section the calculation of the proximity potential is described step by step and is based on [1].
If one considers the nuclear part of the nucleus-nucleus interaction potential which is the proximity potential in this model, one gets

$$V_{nuc}(r) = K\Phi(\zeta) \tag{3.2}$$

The proximity potential is a product of the strength factor K and the dimensionless proximity potential function Φ, which depends on the dimensionless quantity ζ.
ζ is the contact separation in units of the Süssmann measure of the diffuseness of the nuclear surface b [5]

$$\zeta = \frac{s}{b} \tag{3.3}$$

b describes the width of the diffuse surface of the nucleus. It is taken as 1 fm [5].
The density distribution of both nuclei is assumed to be spherical and frozen.

For the calculation some information about the participating nuclei in the fusion reactions is needed: the proton numbers Z_1 and Z_2 as maybe if available the root mean square (rms) charge radii r_{rms} [10]. If the rms charge radii of the two fusing nuclei are not available (because no measurement has been undertaken to estimate their charge radii), then an approximation is used for calculation of the nuclear charge radii.
First the calculation of the strength factor K needs to be done, which is given by

$$K = 4\pi\gamma Cb \tag{3.4}$$

where γ is the mean of the surface tension coefficients according to the two nuclei. The calculation of γ and of the reduced radius C is discussed later on.
The mean of the surface tension coefficients is the energy per surface of an unit sphere and is obtained by

$$\gamma = \frac{a_2}{4\pi {r_0}^2} \tag{3.5}$$

with a_2 as the surface energy coefficient and the nuclear radius constant r_0. This nuclear radius constant has nearly the same value for all nuclei and is derived from the correlation by the correlation that the radius R_{00} of a spherical nucleus is proportional to the cubic root of the mass number A [11] given by

$$R_{00} = r_0 \cdot A^{1/3} \tag{3.6}$$

which is only an approximation, that does not represent the experimentally measured rms radii very well [12]. For the calculation r_0 is taken as 1.14 fm [13] .

The surface energy coefficient can be calculated via

$$a_2 = 18.36\ MeV - \frac{Q\ ({t_1}^2 + {t_2}^2)}{2{r_0}^2} \tag{3.7}$$

and is the average of the values for the two fusing nuclei.
Q describes the neutron skin stiffness coefficient and is a measure of the resistance of neutrons to separate from protons in a nucleus to form a neutron skin [14] and is taken as 35.4 MeV [13]. t describes the neutron skin and has to be determined for each nucleus

$$t = \frac{3}{2}\ r_0\ \frac{J\ I - \frac{1}{12}\ c_1\ Z\ A^{-1/3}}{Q\ +\ \frac{9}{4}\ J\ A^{-1/3}} \tag{3.8}$$

Here J is the symmetric energy coefficient and "represents with a very good accuracy the energy cost per nucleon to convert all protons into neutrons in symmetric infinity nuclear matter at saturation density ρ_0" [14]. It is taken as 32.65 MeV [13], $c_1 = 3e^2/5r_0 = 0.757895\ MeV$ [11], Z the proton numbers and A the mass number of each nuclei.
I is the asymmetric term of a nucleus which describes the symmetry between proton number and neutron number N and is lost for growing mass number of a nucleus because of the repulsive coulomb force [15]. It is given by

$$I = \frac{(N - Z)}{A} \tag{3.9}$$

C is the reduced radius of the two nuclei

$$C = \frac{C_1 C_2}{C_1 + C_2} \tag{3.10}$$

Here C_1 and C_2 are the matter radii of each nuclei. $C_{1,2}$ can be calculated for each nuclei by

$$C = c + \frac{N}{A}\ t \tag{3.11}$$

c is the half-density radius of the charge distribution. It describes "where the nuclear density has dropped to half its central value" [16] and is described by

$$c = R_{00}\ (1 - \frac{7}{2}\frac{b^2}{{R_{00}}^2} - \frac{49}{8}\frac{b^4}{{R_{00}}^4} + ...) \tag{3.12}$$

As already mentioned, equation (3.6) does not provide good results for the experimentally measured rms radii.
In the calculation made by the author there are two possibilities to determine the nuclear charge radius R_{00}, which describes the range of nuclear charge of a deformed nucleus in any direction [12]. These possibilities depend on whether there are experimentally measured rms charge radius values r_{rms} available for the two interacting nuclei or not. If the rms charge radius values exist, the calculation is done by

$$R_{00} = \sqrt{\frac{5}{3}}\ r_{rms} \tag{3.13}$$

This relation follows the approximation ${r_{rms}}^2 = \frac{Q_{00}}{e\ Z}$, with the electric monopole moment of the spherical nucleus $Q_{00} = \frac{3}{5} e Z {R_{00}}^2$ [12].
Otherwise, an approximation for the nuclear charge radii, which takes the neutron excess $N - Z$ of

each corresponding nucleus into account, can be used [12]

$$R_{00} = 1.240\ A^{1/3}\ (1 + \frac{1.646}{A} - 0.191\frac{A-2Z}{A}) \tag{3.14}$$

An investigation on the difference of these two methods is done in the analysis chapter.

All necessary quantities for the calculation of K are derived by the equations above. For calculating the dimensionless proximity potential function Φ, a distinction needs to be made:

$$\Phi(\zeta) = -0.1353 + \sum_{n=0}^{5} \frac{c_n}{n+1}(2.5-\zeta)^{n+1}, \qquad \text{for } \ 0 < \zeta < 2.5 \tag{3.15}$$

$$\Phi(\zeta) = -0.09551 \cdot e^{\frac{(2.75-\zeta)}{0.7176}} \qquad \text{for } \ \zeta > 2.5 \tag{3.16}$$

c_n are constants and have following values:
$c_0 = -0.1886,\ c_1 = -0.2628,\ c_2 = -0.15216,\ c_3 = -0.04562,\ c_4 = 0.069136,\ c_5 = -0.011454.$

The barrier height V_0 of the nucleus-nucleus interaction potential is derived by looking for the extremum of the interaction potential. It is given by

$$-\frac{dV}{dr} = \frac{Z_1 Z_2 e^2}{r^2} + \frac{K}{b}\phi(\zeta) = 0 \tag{3.17}$$

ϕ represents the proximity force function and is the negative derivation of Φ with respect to ζ.

$$\phi = -\frac{d\Phi}{d\zeta} \tag{3.18}$$

The dimensionless proximity force function ϕ are derived from equation (3.15) and equation (3.16)

$$\phi(\zeta) = \sum_{n=0}^{5} c_n(2.5-\zeta)^n, \qquad \text{for } \ 0 < \zeta < 2.5 \tag{3.19}$$

$$\phi(\zeta) = -0.1331 \cdot e^{\frac{(2.75-\zeta)}{0.7176}}, \qquad \text{for } \ \zeta > 2.5 \tag{3.20}$$

3.2 Neck Formation

Fusion reactions of heavy ions at low energies, energies below the coulomb barrier, need more than one degree of freedom, as the predicted values of a one-dimensional model, with the radial separation as the degree of freedom, do not reproduce experimental data very well. The predicted values for the barrier height reach an exceedance of several orders of magnitude [2]. For this an additional degree of freedom, neck formation, is included to lower the overpredicted values towards the experimental data. For the calculation of the neck formation, the multidimensional model by Aguiar et al. [2] was taken. This multidimensional model includes radial separation, neck formation and asymmetry as degrees of freedom. An important condition for neck formation is to assume that both nuclei are not frozen so that deformation for both nuclei at a certain distance is possible.

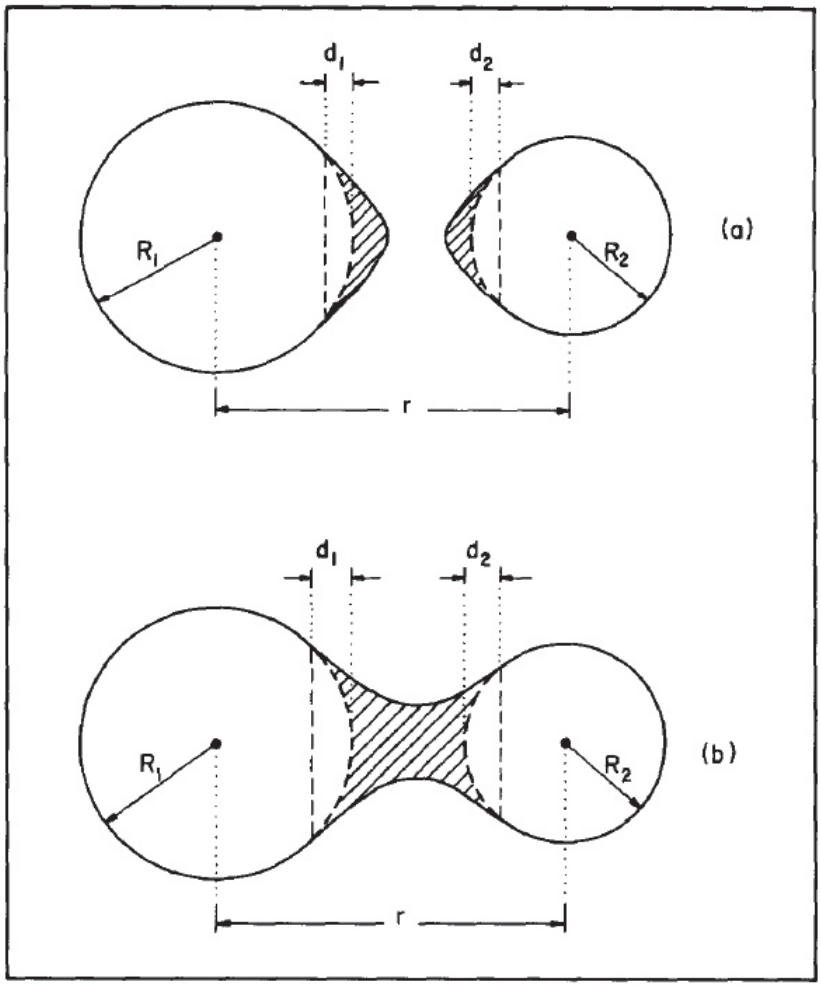

Figure 3.2: Illustration of neck formation for two approaching nuclei. Initial stage when nuclear forces begin to act (a). Nuclear matter of the nuclei overlap (b). [2]

Figure 3.2 (a) illustrates early stages of two colliding nuclei at a separation radius for which the nuclear forces begin to act. The nuclei are still separated. For later stages (figure 3.2 (b)), the nuclear matter of the two colliding nuclei overlap and the two nuclei are not a separate systems any more. The radial separation ρ is

$$\rho = \frac{r}{(R_1 + R_2)} \tag{3.21}$$

In this notation R_1 and R_2 equal the matter radii C_1 and C_2 of the former notation.

The neck formation λ is

$$\lambda = \frac{d_1 + d_2}{(R_1 + R_2)} \tag{3.22}$$

here $d_{1,2}$ are the thickness of the missing spherical tips.
The asymmetry Δ is

$$\Delta = \frac{R_1 - R_2}{R_1 + R_2} \tag{3.23}$$

As the two approaching nuclei deform, their radii need to compensate the deforming volume by changing themselves because of volume conservation.
The system of the colliding nuclei becomes unstable as neck formation sets in. This happens for energies between the critical value V_{neck} and the former barrier height V_0. The difference ΔV describes the energy shift, which is gained by the neck formation and lowers the overestimated predicted values

$$\Delta V_{neck} = V_0 - V_{neck} \tag{3.24}$$

Aguiar et al. [2] investigated the neck formation for symmetric ($\Delta = 0$) and asymmetric fusion systems. They attributed the dependence of the effective barrier decrease ΔV_{neck} to the parameter ζ_{eff}, which is the effective fissility and is defined as

$$\zeta_{eff} = \left(\frac{Z^2}{A}\right)_{eff} = \frac{4 Z_1 Z_2}{{A_1}^{1/3} {A_2}^{1/3} ({A_1}^{1/3} + {A_2}^{1/3})} \tag{3.25}$$

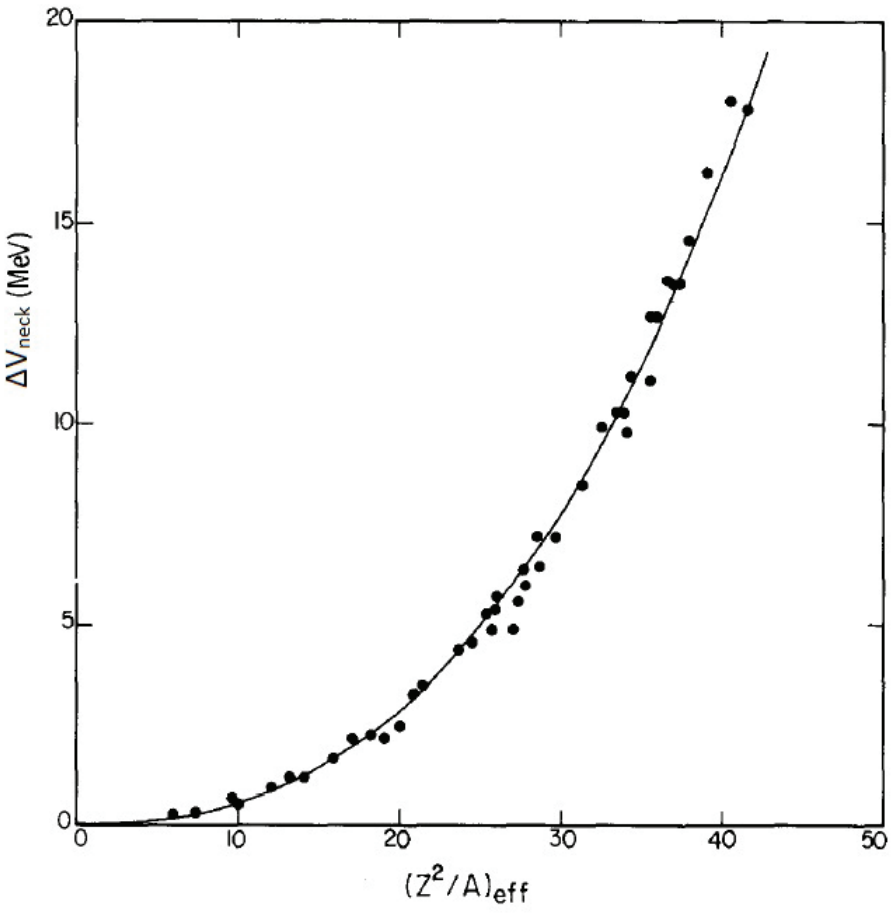

Figure 3.3: Dependence of ΔV_{neck} on the parameter ζ_{eff}. The solid line represents the trend line. Image taken from [2] with y-label named to this paper.

The effective fissility is "a measure of the importance of the repulsive coulomb force compared to the attractive nuclear surface tension" [17].
For Figure 3.3 they got following fit parameters

$$\Delta V_{neck} = \alpha \ {\zeta_{eff}}^{\beta} \tag{3.26}$$

with

$$\alpha \approx 0.0016 \ MeV, \qquad \beta \approx 2.5 \tag{3.27}$$

The original barrier height calculated by the proximity potential V_0 is lowered by the effective barrier decrease ΔV_{neck}.
This model of neck formation is only applicable on sub-barrier fusion reactions, as for fusion processes at high energies the one-dimensional model reproduces acceptable results.

3.3 Extra Push

Fusion processes are regulated by repulsive electric forces and attractive nuclear forces. As mentioned before, the strength of electric force increases with the proton numbers Z_1 Z_2 of the two colliding nuclei. Because of that lighter systems, with lower repulsive electric forces, are supposed to fuse more easily than heavier systems. It is even assumed [3] that the electric repulsion reaches values so that a heavy system starting from rest at contact, the system will reseparate. To make such a heavy system fuse, an additional bombarding energy above the interaction potential barrier is needed. This additional energy is introduced as the extra push and is approximated for central collisions by [3]

$$\Delta V_{extrapush} = \begin{cases} 0 & \text{for } (\frac{Z^2}{A})_{eff} \leq (\frac{Z^2}{A})_{eff\ thr} \\ \\ K[(\frac{Z^2}{A})_{eff} - (\frac{Z^2}{A})_{eff\ thr}]^2 & \text{for } (\frac{Z^2}{A})_{eff} > (\frac{Z^2}{A})_{eff\ thr} \end{cases} \tag{3.28}$$

K is the thud wall stiffness coefficient and is according to [3]

$$K = \frac{{A_1}^{1/3}{A_2}^{1/3}({A_1}^{1/3} + {A_2}^{1/3})^2}{A_1 + A_2} \frac{32}{2025} (\frac{3}{\pi})^{\frac{2}{3}} (\frac{e^2}{\hbar c})^2 mc^2 a^2 \tag{3.29}$$

$(\frac{Z^2}{A})_{eff}$ is the effective fissility. $(\frac{Z^2}{A})_{effthr}$ and a are numerical constants, which are determined either from experiment or model calculations. a is the thud wall slope coefficient. m is the nuclear mass unit ($m = 931\ MeV/c^2$).
For the calculation experimentally determined values were used

$$(\frac{Z^2}{A})_{eff\ thr} \approx 33, \qquad a \approx 12 \tag{3.30}$$

The already neck-formation-corrected barrier height is lifted by the extra push energy $\Delta V_{extrapush}$, which leads to a new barrier height V_{corr}

$$V_{corr} = V_{neck} + \Delta V_{extrapush} \tag{3.31}$$

Only for heavy systems $(\frac{Z^2}{A})_{eff} > (\frac{Z^2}{A})_{eff\ thr}$ will the extra push be different from zero and counteract fusion processes.

4 Fusion Cross Section and Excitation Function

The aim of this work is to get to know the probability of fusion processes for two arbitrary colliding nuclei. The fusion cross section is a measure of the probability of a fusion reaction.
A calculation according to K. Siwek-Wilczyńska et al. (2004) [4] requires a barrier height distribution $p(V)$. This assumption is necessary to account for the influence of additional different degrees of freedom (e. g. vibration, rotation, etc.). The assumed distribution is modelled by a Gaussian distribution

$$p(V) = \frac{1}{w\sqrt{2\pi}} e^{-\frac{(V-V_0)^2}{2w^2}} \tag{4.1}$$

here $p(V)$ is the distribution of the barrier heights, V_0 is the mean barrier height, for which V_{corr} from equation (3.31) is used, and w is the barrier height distribution.
By using the classical expression for the fusion cross section

$$\sigma_{fus} = \pi {R_\sigma}^2 (1 - \frac{V}{E}) \qquad \text{for} \quad E > V \tag{4.2}$$

and by combining equation (4.1) with equation (4.2), one gets the following expression [4] for the fusion cross section, which is used for the determination of the excitation function

$$\sigma_{fus} = \pi {R_\sigma}^2 \frac{w}{E\sqrt{2\pi}} [X\sqrt{\pi}(1 + erf\ X) + e^{-X^2}] \tag{4.3}$$

with

$$X = \frac{E - V_0}{\sqrt{2}w} \tag{4.4}$$

R_σ approximates the location of the maximum barrier height [4] and is determined by equation (3.17). $erf\ X$ is the gaussion error function.
The barrier height distribution is given by

$$w = \sqrt{{w^2}_{tunnel} + {w^2}_{stat,1} + {w^2}_{stat,2} + {w^2}_{vibr,1} + {w^2}_{vibr,2}} \tag{4.5}$$

Equation (4.5) represents the total barrier height distribution of the fusing system and takes quantum effects of subbarrier tunneling as static quadrupole deformations and surface vibrations of the participating nuclei into account.
The values of the distribution barrier height distribution w for the determination of the fusion cross sections and its excitation functions for each fusion reaction, were taken from [4].

5 Results and Analysis

The calculated results for the barrier height and its location radius are listed step by step. For analysis, the fitted values $V_{0,fit}$, $R_{0,fit}$, the width of the barrier height distribution w_{fit}, as well as the theoretically determined width of the barrier height distribution w_{theo} are taken from [4] and are listed in table 5.1.
The fusion reactions are listed in order of the increasing coulomb barrier parameter z, which is a measure of the coulomb barrier and is given by

$$z = \frac{Z_1 Z_2}{(A^{1/3} + A^{1/3})} \tag{5.1}$$

For the analysis, a distinction into three groups is made [4]:

- light systems: $z < 70$
- medium systems: $70 \leq z \leq 130$
- heavy systems: $z > 130$

Table 5.1: Fitted values of the barrier height V_0 and its location radius R_0, the width of the barrier height distribution w_{fit}, as well as the theoretically determined width of the barrier height distribution w_{theo}.

Reaction	z	$V_{0,fit}$ [MeV]	$R_{0,fit}$ [fm]	w_{fit} [MeV]	w_{theo} [MeV]
^{48}Ca + ^{48}Ca	55.03	51.2	11.2	1.11	1.25
^{30}Si + ^{64}Ni	55.16	51.4	9.6	1.38	1.39
^{30}Si + ^{62}Ni	55.48	52.1	9.7	1.55	1.42
^{28}Si + ^{64}Ni	55.71	50.4	7.6	1.12	1.43
^{28}Si + ^{62}Ni	56.04	51.3	7.7	1.20	1.46
^{30}Si + ^{58}Ni	56.18	52.8	8.8	1.59	1.36
^{40}Ca + ^{48}Ca	56.70	51.8	11.5	1.78	1.31
^{28}Si + ^{58}Ni	56.75	52.9	8.1	1.32	1.41
^{40}Ca + ^{44}Ca	57.55	51.8	7.9	1.59	1.35
^{40}Ca + ^{40}Ca	58.48	53.6	9.5	1.60	1.40
^{36}S + ^{64}Ni	61.35	56.8	8.5	1.17	1.46
^{34}S + ^{64}Ni	61.88	56.9	8.5	1.25	1.48
^{40}Ca + ^{50}Ti	61.94	57.3	9.4	1.72	1.40
^{40}Ca + ^{48}Ti	62.37	57.1	9.4	1.50	1.42
^{32}S + ^{64}Ni	62.44	57.3	8.1	1.57	1.52
^{36}S + ^{58}Ni	62.46	58.4	7.7	1.53	1.42
^{40}Ca + ^{46}Ti	62.83	57.3	9.4	1.45	1.44
^{16}O + ^{154}Sm	62.94	58.4	9.6	2.25	2.38
^{34}S + ^{58}Ni	63.01	58.5	7.6	1.25	1.45

Table 5.1 – continued from previous page

Reaction	z	$V_{0,fit}$ [MeV]	$R_{0,fit}$ [fm]	w_{fit} [MeV]	w_{theo} [MeV]
^{17}O + ^{144}Sm	63.49	60.6	10.8	2.06	1.59
^{16}O + ^{148}Sm	63.51	59.4	10.2	1.98	1.93
^{32}S + ^{58}Ni	63.59	59.6	8.3	1.35	1.48
^{16}O + ^{144}Sm	63.91	60.5	10.3	1.45	1.64
^{16}O + ^{186}W	71.95	68.3	10.6	2.29	2.43
^{16}O + ^{208}Pb	77.68	73.6	10.5	1.57	1.72
^{36}S + ^{96}Zr	81.21	74.9	11.0	1.34	2.31
^{36}S + ^{90}Zr	82.23	77.0	10.8	1.24	1.60
^{36}S + ^{110}Pd	90.94	85.5	8.2	1.91	2.61
^{32}S + ^{110}Pd	92.39	86.3	8.0	2.63	2.65
^{64}Ni + ^{64}Ni	98.00	92.7	7.8	1.58	2.07
^{58}Ni + ^{64}Ni	99.61	94.6	6.5	2.18	1.97
^{40}Ca + ^{96}Zr	100.01	93.6	9.3	2.65	2.79
^{58}Ni + ^{60}Ni	100.70	96.6	7.5	1.93	1.87
^{40}Ca + ^{90}Zr	101.25	96.1	10.0	1.53	1.90
^{58}Ni + ^{58}Ni	101.27	95.8	6.0	1.18	1.88
^{40}Ar + ^{122}Sn	107.40	103.6	9.8	2.58	1.94
^{40}Ar + ^{116}Sn	108.47	103.3	8.7	2.23	1.98
^{40}Ar + ^{112}Sn	109.22	104.0	8.9	2.26	2.01
^{64}Ni + ^{74}Ge	109.29	103.2	6.5	1.97	3.09
^{58}Ni + ^{74}Ge	111.04	106.8	7.0	2.96	3.05
^{40}Ca + ^{124}Sn	118.95	113.4	9.6	2.75	2.13
^{28}Si + ^{198}Pt	123.18	120.9	9.8	3.41	2.94
^{34}S + ^{168}Er	124.24	121.5	10.3	4.21	4.55
^{40}Ar + ^{154}Sm	127.11	121.0	7.3	3.40	4.27
^{40}Ar + ^{148}Sm	128.14	124.7	8.5	3.15	3.15
^{40}Ar + ^{144}Sm	128.85	124.4	8.3	2.19	2.31
^{40}Ca + ^{192}Os	165.42	167.9	10.7	5.46	4.18
^{40}Ca + ^{194}Pt	169.40	171.0	9.6	4.12	4.20

The run of the nucleus-nucleus interaction potential and its quantities are calculated as well as each excitation function for every fusion reaction is determined.
Every section includes a further step of modification to the nucleus-nucleus interaction potential. Comparisons between the results of these calculations and fitted data are made.

5.1 Calculation of the nucleus-nucleus interaction potential by the proximity potential

Here the run for the nucleus-nucleus interaction potential for each reaction is determined by using equations (3.1)-(3.20).
The results are listed in table (5.2).

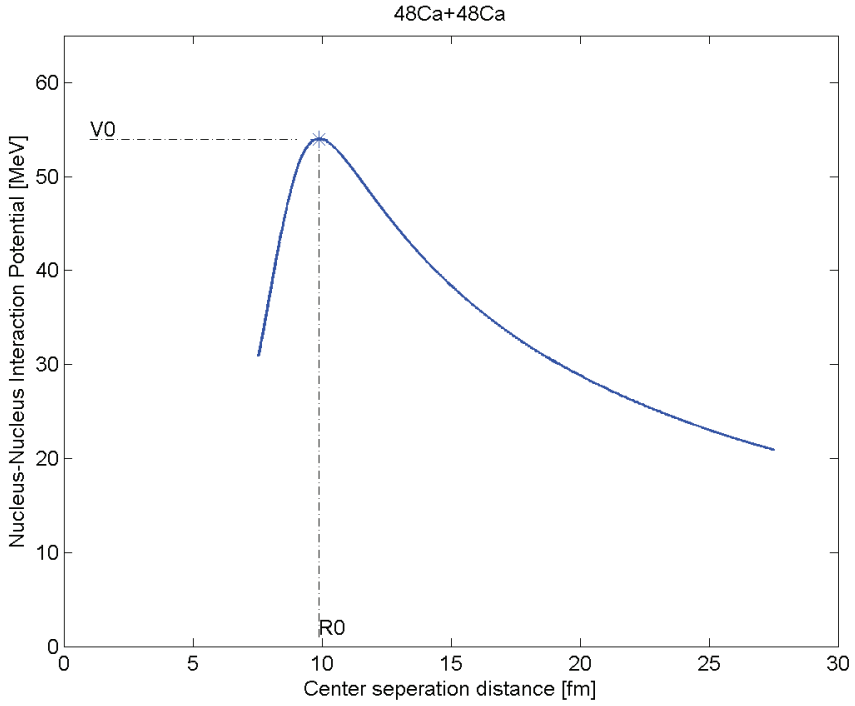

Figure 5.1: Nucleus-nucleus interaction potential for the light fusion reaction ($z = 55.03$) $^{48}Ca + ^{48}Ca$ with a determined barrier height of $V_0 = 54.5125\ MeV$ and a location radius of $R_\sigma = 9.7854\ fm$.

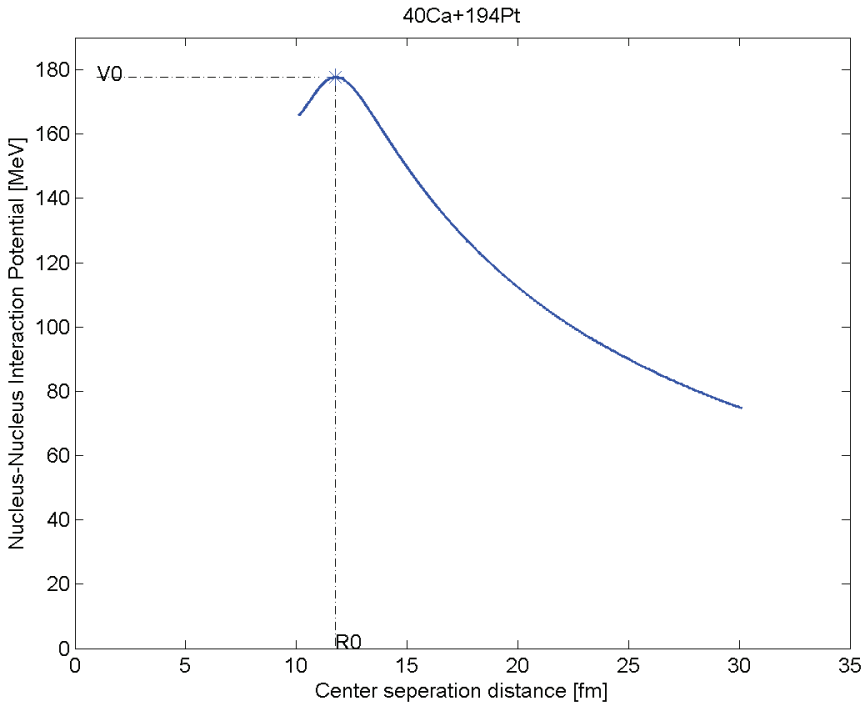

Figure 5.2: Nucleus-nucleus interaction potential for the heavy fusion reaction ($z = 169.40$) $^{40}Ca + ^{194}Pt$ with a determined barrier height of $V_0 = 175.3262\ MeV$ and a location radius of $R_\sigma = 11.9527\ fm$.

Table 5.2: Values for the calculated barrier height V_0 and its location radius R_0 versus the fitted data.

Reaction	V_0 [MeV]	R_0 [fm]	$V_{0,fit}$ [MeV]	$R_{0,fit}$ [fm]
^{48}Ca + ^{48}Ca	54.5125	9.7854	51.2	11.2
^{30}Si + ^{64}Ni	53.6280	9.7409	51.4	9.6
^{30}Si + ^{62}Ni	53.8986	9.6855	52.1	9.7
^{28}Si + ^{64}Ni	53.9683	9.6794	50.4	7.6
^{28}Si + ^{62}Ni	54.2427	9.6241	51.3	7.7
^{30}Si + ^{58}Ni	54.7699	9.5193	52.8	8.8
^{40}Ca + ^{48}Ca	55.0506	9.6825	51.8	11.5
^{28}Si + ^{58}Ni	55.1254	9.4479	52.9	8.1
^{40}Ca + ^{44}Ca	54.8733	9.7100	51.8	7.9
^{40}Ca + ^{40}Ca	55.6010	9.5697	53.6	9.5
^{36}S + ^{64}Ni	59.7555	10.0159	56.8	8.5
^{34}S + ^{64}Ni	60.1041	9.9541	56.9	8.5
^{40}Ca + ^{50}Ti	60.0840	9.7636	57.3	9.4
^{40}Ca + ^{48}Ti	59.9869	9.7736	57.1	9.4
^{32}S + ^{64}Ni	60.5981	9.8560	57.3	8.1
^{36}S + ^{58}Ni	60.9945	9.7944	58.4	7.7
^{40}Ca + ^{46}Ti	59.9778	9.7829	57.3	9.4
^{16}O + ^{154}Sm	61.9827	10.7406	58.4	9.6
^{34}S + ^{58}Ni	61.3585	9.7226	58.5	7.6
^{17}O + ^{144}Sm	63.6177	10.4389	60.6	10.8

Table 5.2 – continued from previous page

Reaction	V_0 [MeV]	R_0 [fm]	$V_{0,fit}$ [MeV]	$R_{0,fit}$ [fm]
^{16}O + ^{148}Sm	63.1146	10.5297	59.4	10.2
^{32}S + ^{58}Ni	61.8751	9.6345	59.6	8.3
^{16}O + ^{144}Sm	63.7394	10.4228	60.5	10.3
^{16}O + ^{186}W	72.1183	11.0291	68.3	10.6
^{16}O + ^{208}Pb	79.0870	11.1492	73.6	10.5
^{36}S + ^{96}Zr	80.6791	10.6339	74.9	11.0
^{36}S + ^{90}Zr	81.9731	10.4480	77.0	10.8
^{36}S + ^{110}Pd	90.5498	10.9120	85.5	8.2
^{32}S + ^{110}Pd	91.7284	10.7521	86.3	8.0
^{64}Ni + ^{64}Ni	98.6308	10.6491	92.7	7.8
^{58}Ni + ^{64}Ni	100.5683	10.4175	94.6	6.5
^{40}Ca + ^{96}Zr	99.9188	10.7274	93.6	9.3
^{58}Ni + ^{60}Ni	101.7305	10.2806	96.6	7.5
^{40}Ca + ^{90}Zr	101.5133	10.5415	96.1	10.0
^{58}Ni + ^{58}Ni	102.5908	10.1860	95.8	6.0
^{40}Ar + ^{122}Sn	108.3829	11.1506	103.6	9.8
^{40}Ar + ^{116}Sn	109.2604	11.0533	103.3	8.7
^{40}Ar + ^{112}Sn	109.9748	10.9757	104.0	8.9
^{64}Ni + ^{74}Ge	109.8822	10.9392	103.2	6.5
^{58}Ni + ^{74}Ge	111.9858	10.7077	106.8	7.0
^{40}Ca + ^{124}Sn	120.7113	11.1095	1134	9.6
^{28}Si + ^{198}Pt	126.7314	11.5835	120.9	9.8
^{34}S + ^{168}Er	125.3432	11.6891	121.5	10.3
^{40}Ar + ^{154}Sm	128.1273	11.7347	121.0	7.3
^{40}Ar + ^{148}Sm	130.2827	11.5138	124.7	8.5
^{40}Ar + ^{144}Sm	131.4711	11.4069	124.4	8.3
^{40}Ca + ^{192}Os	170.7431	11.9619	167.9	10.7
^{40}Ca + ^{194}Pt	175.3262	11.9527	171.0	9.6

As can be seen, the barrier heights increase towards heavy systems and their location radii shift outward. The increase of the barrier height for heavy systems is because of the increase of the repulsive coulomb force for increasing proton numbers.
The barrier heights calculated by the proximity model overestimate the fitted data for all 48 reactions.

5.2 Correction by the neck formation

On the calculated barrier height by the proximity model, neck formation was included. This lead to a lowering of the barrier heights, as can be seen in table 5.3.

Table 5.3: Values for the effective barrier decrease by neck formation ΔV_{neck} and corrected barrier height V_{neck}

Reaction	ΔV_{neck} [MeV]	V_{neck} [MeV]
^{48}Ca + ^{48}Ca	1.8144	52.6981
^{30}Si + ^{64}Ni	2.1240	51.5040
^{30}Si + ^{62}Ni	2.2136	51.6851
^{28}Si + ^{64}Ni	2.3066	51.6617
^{28}Si + ^{62}Ni	2.4042	51.8385
^{30}Si + ^{58}Ni	2.4137	52.3562
^{40}Ca + ^{48}Ca	2.2762	52.7744
^{28}Si + ^{58}Ni	2.6224	52.5030
^{40}Ca + ^{44}Ca	2.5399	52.3333
^{40}Ca + ^{40}Ca	2.8622	52.7389
^{36}S + ^{64}Ni	2.3812	57.3743
^{34}S + ^{64}Ni	2.5515	57.5526
^{40}Ca + ^{50}Ti	2.7434	57.3406
^{40}Ca + ^{48}Ti	2.8887	57.0983
^{32}S + ^{64}Ni	2.7447	57.8534
^{36}S + ^{58}Ni	2.7027	58.2918
^{40}Ca + ^{46}Ti	3.0480	56.9299
^{16}O + ^{154}Sm	2.4005	59.5822
^{34}S + ^{58}Ni	2.8971	58.4614
^{17}O + ^{144}Sm	2.4658	61.1519
^{16}O + ^{148}Sm	2.5377	60.5768
^{32}S + ^{58}Ni	3.1178	58.7574
^{16}O + ^{144}Sm	2.6367	61.1027
^{16}O + ^{186}W	2.8650	69.2533
^{16}O + ^{208}Pb	3.1615	75.9254
^{36}S + ^{96}Zr	3.4236	77.2555
^{36}S + ^{90}Zr	3.7269	78.2462
^{36}S + ^{110}Pd	4.0557	86.4941
^{32}S + ^{110}Pd	4.6546	87.0739
^{64}Ni + ^{64}Ni	4.7537	93.8771
^{58}Ni + ^{64}Ni	5.3744	95.1939
^{40}Ca + ^{96}Zr	5.2782	94.6406
^{58}Ni + ^{60}Ni	5.8277	95.9029
^{40}Ca + ^{90}Zr	5.7432	95.7701
^{58}Ni + ^{58}Ni	6.0802	96.5106
^{40}Ar + ^{122}Sn	5.1657	103.2172
^{40}Ar + ^{116}Sn	5.5227	103.7378
^{40}Ar + ^{112}Sn	5.7849	104.1899

Table 5.3 – continued from previous page

Reaction	ΔV_{neck} [MeV]	V_{neck} [MeV]
^{64}Ni + ^{74}Ge	5.5320	104.3502
^{58}Ni + ^{74}Ge	6.2481	105.7377
^{40}Ca + ^{124}Sn	6.5789	114.1324
^{28}Si + ^{198}Pt	6.5429	120.1885
^{34}S + ^{168}Er	6.5199	118.8233
^{40}Ar + ^{154}Sm	6.4819	121.6454
^{40}Ar + ^{148}Sm	6.8366	123.4461
^{40}Ar + ^{144}Sm	7.0920	124.3791
^{40}Ca + ^{192}Os	10.4211	160.3220
^{40}Ca + ^{194}Pt	10.9650	164.3612

5.3 Correction by the extra push

The Extra push was also applied to the barrier height of the proximity model. The extra push only matters for "heavier" systems ($z > 100$), as the extra push energy $\Delta V_{extrapush}$ is zero for lighter systems. Results are listed in table 5.4.

Table 5.4: Values for the extra push energy $\Delta V_{extrapush}$ and the neck formation and extra push corrected barrier height $V_{extrapush}$

Reaction	$\Delta V_{extrapush}$ [MeV]	$V_{extrapush}$ [MeV]
^{48}Ca + ^{48}Ca	0	52.6981
^{30}Si + ^{64}Ni	0	51.5040
^{30}Si + ^{62}Ni	0	51.6851
^{28}Si + ^{64}Ni	0	51.6617
^{28}Si + ^{62}Ni	0	51.8385
^{30}Si + ^{58}Ni	0	52.3562
^{40}Ca + ^{48}Ca	0	52.7744
^{28}Si + ^{58}Ni	0	52.5030
^{40}Ca + ^{44}Ca	0	52.3333
^{40}Ca + ^{40}Ca	0	52.7389
^{36}S + ^{64}Ni	0	57.3743
^{34}S + ^{64}Ni	0	57.5526
^{40}Ca + ^{50}Ti	0	57.3406
^{40}Ca + ^{48}Ti	0	57.0983
^{32}S + ^{64}Ni	0	57.8534
^{36}S + ^{58}Ni	0	58.2918
^{40}Ca + ^{46}Ti	0	56.9299
^{16}O + ^{154}Sm	0	59.5822
^{34}S + ^{58}Ni	0	58.4614
^{17}O + ^{144}Sm	0	61.1519
^{16}O + ^{148}Sm	0	60.5768
^{32}S + ^{58}Ni	0	58.7574
^{16}O + ^{144}Sm	0	61.1027
^{16}O + ^{186}W	0	69.2533
^{16}O + ^{208}Pb	0	75.9254
^{36}S + ^{96}Zr	0	77.2555
^{36}S + ^{90}Zr	0	78.2462
^{36}S + ^{110}Pd	0	86.4941
^{32}S + ^{110}Pd	0	87.0739
^{64}Ni + ^{64}Ni	0	93.8771
^{58}Ni + ^{64}Ni	0	95.1939
^{40}Ca + ^{96}Zr	0	94.6406
^{58}Ni + ^{60}Ni	0.0497	95.9525
^{40}Ca + ^{90}Zr	0.0252	95.7953
^{58}Ni + ^{58}Ni	0.1574	96.6680
^{40}Ar + ^{122}Sn	0	103.2172
^{40}Ar + ^{116}Sn	0	103.7978

Table 5.4 – continued from previous page

Reaction	$\Delta V_{extrapush}$ [MeV]	$V_{extrapush}$ [MeV]
^{40}Ar + ^{112}Sn	0.0352	104.2251
^{64}Ni + ^{74}Ge	0.0001	104.3504
^{58}Ni + ^{74}Ge	0.2696	106.0073
^{40}Ca + ^{124}Sn	0.5042	114.6366
^{28}Si + ^{198}Pt	0.3955	120.5840
^{34}S + ^{168}Er	0.4177	119.2410
^{40}Ar + ^{154}Sm	0.4166	122.0621
^{40}Ar + ^{148}Sm	0.7544	124.2005
^{40}Ar + ^{144}Sm	1.0509	125.4300
^{40}Ar + ^{192}Os	7.7462	168.0682
^{40}Ar + ^{194}Pt	9.2212	173.5823

5.4 Excitation functions

As can be observed in the following figures, the excitation function of the proximity potential underestimates the experimental data. For light and medium fusion reaction, the neck formation corrected barrier height reproduces acceptable results for the excitation function. But for heavy systems the excitation function overestimates the experimental data, as can be seen in figure 5.5 and figure 5.7. This overestimation is minimised by the extra push to preferable values (figure 5.5).
In the following figures $\sigma_{neckformation}$ is the by neck formation corrected proximity potential. $\sigma_{extrapush}$ describes the modification of the proximity potential by neck formation and extra push.
In the following figures (5.3, 5.4 and 5.6) is the extra push energy $\Delta V_{extrapush} = 0$ (as can be seen in table 5.4) and therefore no distinction in $\sigma_{neckformation}$ and $\sigma_{extrapush}$ can be observed.

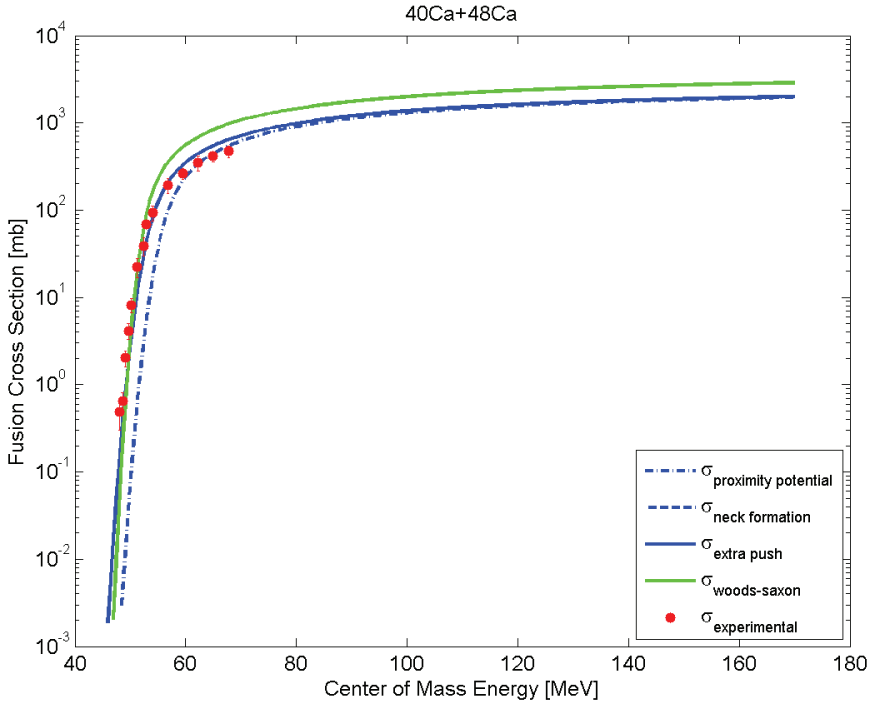

Figure 5.3: Excitation function for the light fusion reaction ($z = 55.03$) $^{40}Ca + ^{48}Ca$ for all calculated models as well as for the woods-saxon potential (distributed barrier potential) by [4] in comparison to experimental data [19]. In this case the excitation functions were determined using rms radii of the two nuclei.

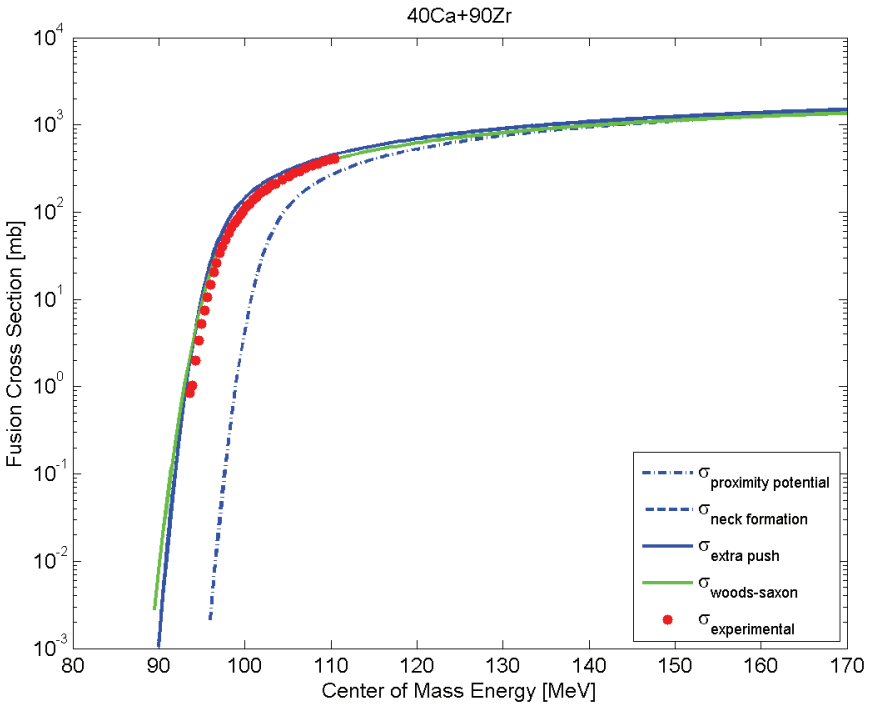

Figure 5.4: Excitation function for the medium fusion reaction ($z = 101.25$) $^{40}Ca + ^{90}Zr$ for all calculated models as well as for the woods-saxon potential (distributed barrier potential) by [4] in comparison to experimental data [20]. In this case the excitation functions were determined using rms radii of the two nuclei.

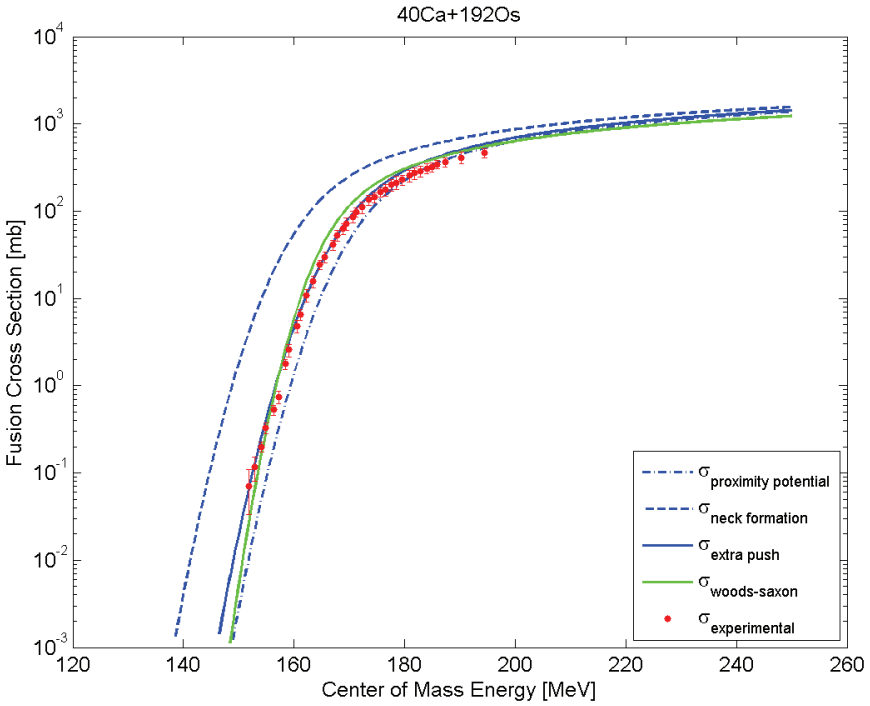

Figure 5.5: Excitation function for the heavy fusion reaction ($z = 165.42$) $^{40}Ca + ^{192}Os$ for all calculated models as well as for the woods-saxon potential (distributed barrier potential) by [4] in comparison to experimental data [21]. In this case the excitation functions were determined using rms radii of the two nuclei.

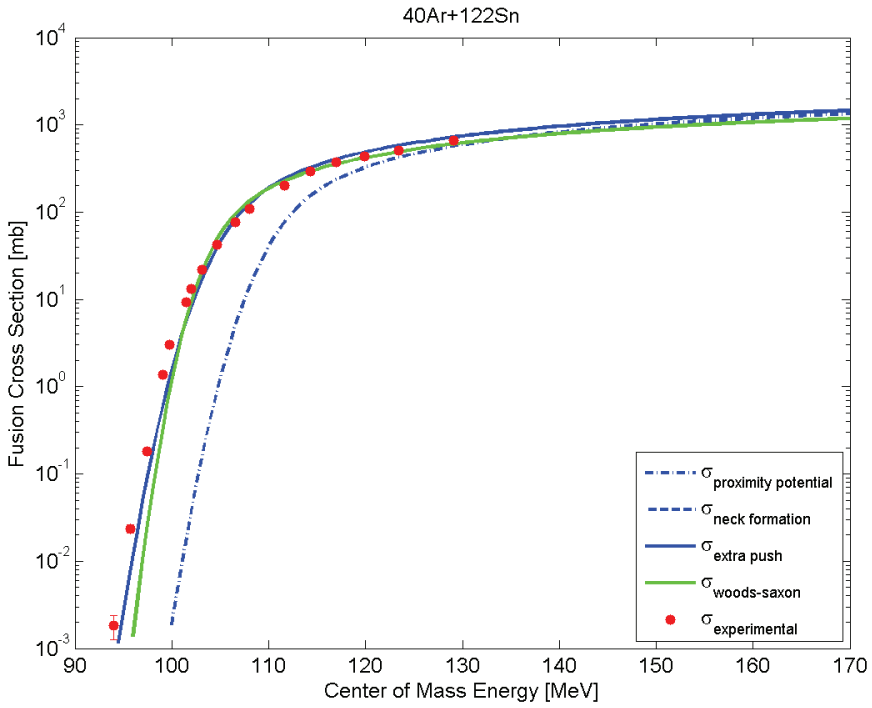

Figure 5.6: Excitation function for the medium fusion reaction ($z = 107.40$) $^{40}Ar + ^{122}Sn$ for all calculated models as well as for the woods-saxon potential (distributed barrier potential) by [4] in comparison to experimental data [22]. In this case the nuclear charge radii of the two nuclei were calculated by using equation (3.14).

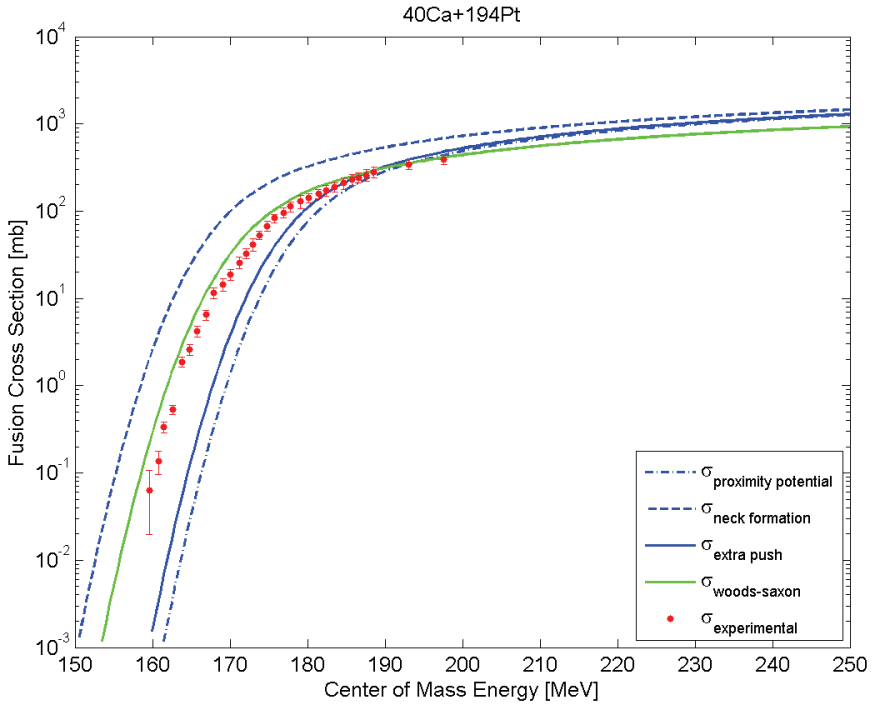

Figure 5.7: Excitation functions for the heavy fusion reaction ($z = 169.40$) $^{40}Ca + ^{194}Pt$ for all calculated models as well as for the woods-saxon potential (distributed barrier potential) by [4] in comparison to experimental data [21]. In this case the nuclear charge radii of the two nuclei were calculated by using equation (3.14).

5.5 Analysis

5.5.1 Analysis of the different models

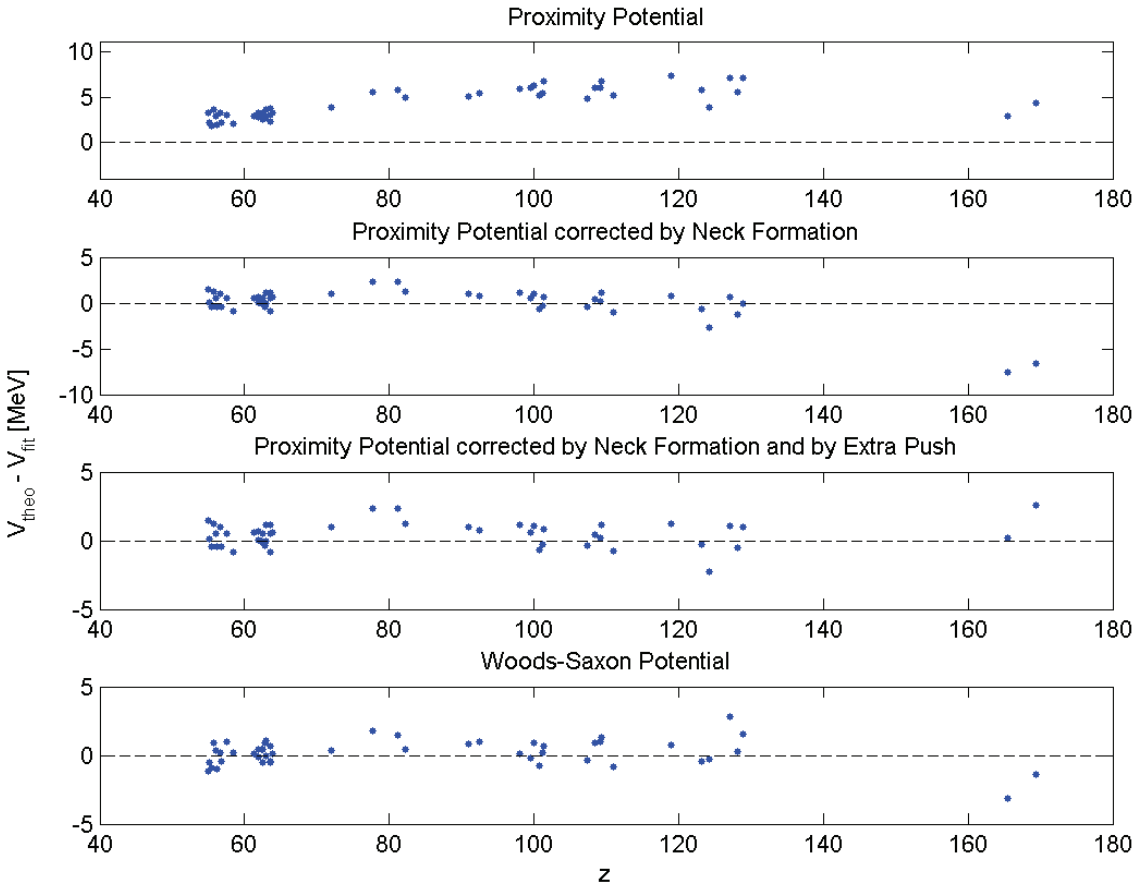

Figure 5.8: Comparison of the theoretically determined barrier heights V_0 and fitted barrier heights V_{fit} for different modifications of the proximity potential in dependence of the coulomb barrier parameter $z = \frac{Z_1 Z_2}{(A^{1/3}+A^{1/3})}$.

Overestimations of fitted data up to a maximum of 7.4 MeV are observed in the original model of the proximity potential. As can be seen in figure 5.8 the difference $V_{theo} - V_{fit}$ increases with the growing coulomb barrier parameter z.

The modification of the proximity potential by the neck formation lowers this overestimation to acceptable discrepancies for light and medium systems ($z \leqslant 130$). For all reactions this model produces discrepancies of about 1.1 MeV on average. But for heavy systems ($z > 130$), for which only two reactions have been analysed, an underestimation of about 7.6 MeV is reached by this step.

For these two heavy systems ($z \gtrsim 110$) the extra push steps in. This leads to an excellent agreement of the theoretical predicted values with the fitted data even for heavier systems. Barrier heights, calculated by this model, show a maximal total deviation of about 2.6 MeV. An improvement of the overestimated data is observed.

In comparison to other introduced models for the nuclear potential, such as the woods-saxon model [4], a decrease in the deviation for heavy systems is observed. The woods-saxon model shows a maximal discrepancy of about 3.2 MeV for the studied systems.

As the original, unmodified proximity potential features discrepancies up to 7.4 MeV, the modifications lower the discrepancies even for heavy systems to a preferable 2.6 MeV.

For the analysis of the results, the mean of the absolute deviation $\overline{\triangle V}$ is calculated by

$$\overline{\triangle V} = \frac{1}{N}\sum_{i=1}^{N}\Delta V_i = \frac{1}{N}\sum_{i=1}^{N} \mid V_i - V_{fit} \mid \tag{5.2}$$

with N as the number of reactions.
The deviation of the single value is given by

$$\sigma = \sqrt{\frac{1}{N-1}\sum_{i=1}^{N}\left(\Delta V_i - \overline{\triangle V}\right)^2} \tag{5.3}$$

The standard deviation of the mean value is determined by

$$\sigma_m = \frac{\sigma}{\sqrt{N}} \tag{5.4}$$

Table 5.5: Values of the mean deviation $\overline{\triangle V}$ to the fitted data, the deviation of the single value σ and the standard deviation of the mean value σ_m are listed for all models as well as for the woods-saxon potential based on [4]. A distinction is made between light, medium and heavy reactions.

	$V_{proximity}$	$V_{neck\ formation}$	$V_{extra\ push}$	$V_{Woods-Saxon}$
$z < 70$				
$\overline{\triangle V}$ $[MeV]$	2.8461	0.5966	0.5966	0.5461
σ $[MeV]$	0.5460	0.4170	0.4170	0.3435
σ_m $[MeV]$	0.1139	0.0870	0.0870	0.0716
$70 \leqslant z \leqslant 130$				
$\overline{\triangle V}$ $[MeV]$	5.6117	0.9610	0.9698	0.8138
σ $[MeV]$	1.0383	0.6642	0.6041	0.6278
σ_m $[MeV]$	0.2119	0.1356	0.1233	0.1281
$z > 130$				
$\overline{\triangle V}$ $[MeV]$	3.5846	7.1084	1.3753	2.2500
σ $[MeV]$	1.0487	0.6641	1.7070	1.2021
σ_m $[MeV]$	0.7415	0.4696	1.2070	0.8500
all 48 reactions				
$\overline{\triangle V}$ $[MeV]$	4.2515	1.0500	0.8155	0.7600
σ $[MeV]$	1.6122	1.4032	0.6083	0.6230
σ_m $[MeV]$	0.2327	0.2025	0.0878	0.0899

As already mentioned the proximity potential overestimates the barrier height for all reactions by

about 5.5%.
The correction by neck formation lowers the mean deviation for light and medium reactions $\overline{\triangle V}$ to acceptable values, whereas for the two heavy fusion reactions a deviation of $\overline{\triangle V} = 7.1084 \pm 0.4696\ MeV$ is reached. But for all 48 reactions it shows a mean absolute deviation $\overline{\triangle V} = 1.0500 \pm 0.2025\ MeV$, which is about 1.2%.
The modification by the extra push shows no change for light systems, because $\Delta V_{extra\ push} = 0$. For medium fusion reactions, a change for the worse is noticed. But for the two heavy systems a significant improvement in the mean deviation $\overline{\triangle V} = 1.3753 \pm 1.2070\ MeV$ is reached. For all 48 reactions the modified proximity potential shows an absolute average deviation of about 1.1%.

5.5.2 Comparison of calculated data with and without rms radii

A comparison of the barrier heights $V_{extrapush}$ by using rms radii and by using the approximation for no rms radii given (equation 3.14) is made.

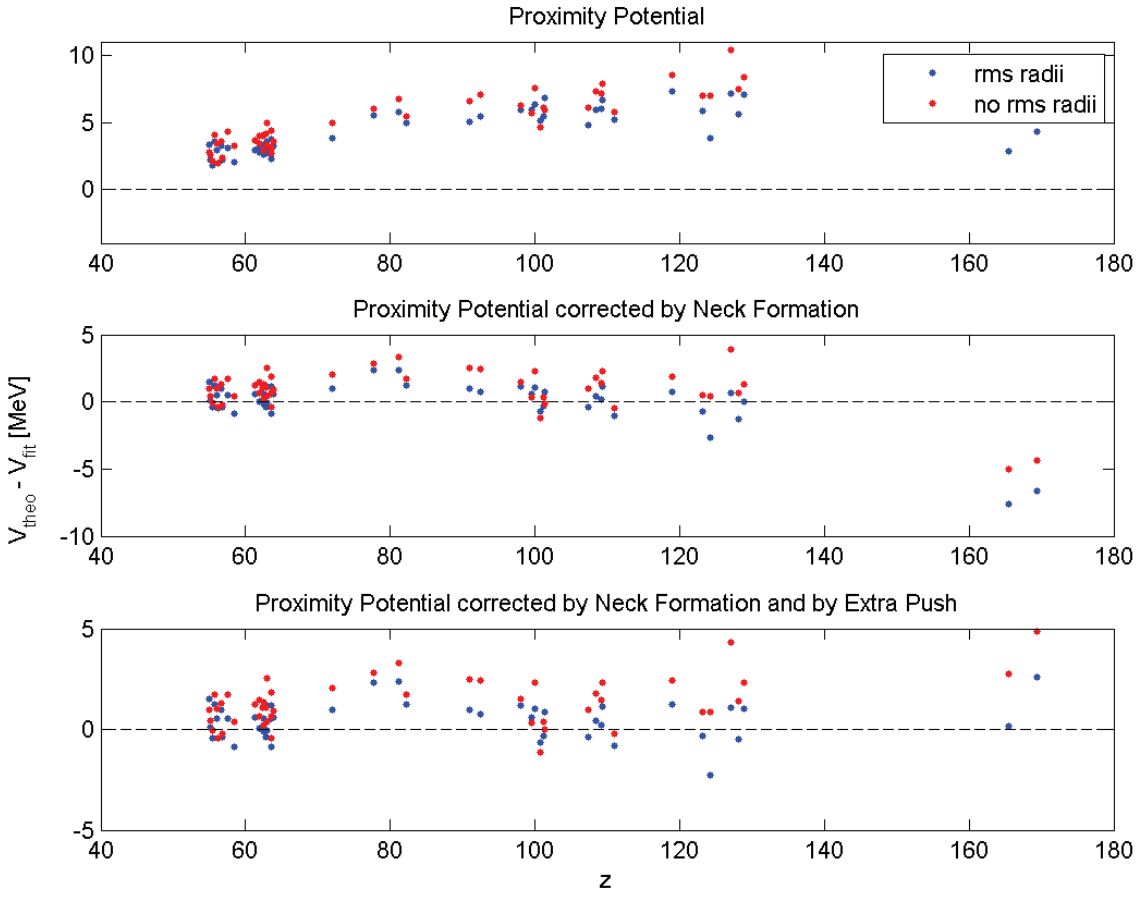

Figure 5.9: Deviation of these theoretically determined barrier heights from the fitted barrier heights.

Table 5.6: Values of the mean deviation $\overline{\triangle V}$ to the fitted data, the deviation of the single value σ and the standard deviation of the mean value σ_m are listed for all models using equation (3.14) as well as for the woods-saxon potential based on [4].

	$V_{proximity}$	$V_{neck\ formation}$	$V_{extra\ push}$	$V_{Woods-Saxon}$
$z < 70$				
$\overline{\triangle V}$ $[MeV]$	3.4206	0.9688	0.9688	0.5461
σ $[MeV]$	0.7659	0.6295	0.6295	0.3435
σ_m $[MeV]$	0.1597	0.1313	0.1313	0.0716
$70 \leqslant z \leqslant 130$				
$\overline{\triangle V}$ $[MeV]$	6.6442	1.5521	1.6824	0.8138
σ $[MeV]$	1.4115	1.0141	1.0509	0.6278
σ_m $[MeV]$	0.2881	0.2070	0.2145	0.1281

Table 5.6 – continued from previous page

	$V_{proximity}$	$V_{neck\ formation}$	$V_{extra\ push}$	$V_{Woods-Saxon}$
$z > 130$				
$\overline{\triangle V}\ [MeV]$	6.0220	4.6710	3.8127	2.2500
$\sigma\ [MeV]$	0.8309	0.4463	1.4893	1.2021
$\sigma_m\ [MeV]$	0.5876	0.3156	1.0531	0.8500
all 48 reactions				
$\overline{\triangle V}\ [MeV]$	5.1375	1.4152	1.4447	0.7600
$\sigma\ [MeV]$	1.9615	1.1164	1.0705	0.6230
$\sigma_m\ [MeV]$	0.2831	0.1611	0.1545	0.0899

As can be seen in figure 5.9, the deviation for the theoretical data using equation (3.14) is stronger than for the theoretical data using the rms radii. Furthermore a change for the worse in the mean deviation is observed. For the neck formation and extra push corrected barrier heights for all 48 reactions the mean absolute deviation by using rms radii is $\overline{\triangle V} = 0.8155 \pm 0.0878\ MeV$ and rises to $\overline{\triangle V} = 1.447 \pm 0.1545\ MeV$ for the approximation by equation (3.14), which is an average deviation of about 1.8%.

The percentage difference of the approximated nuclear charge radii ΔR_{00}, calculated by equation (3.14), and the nuclear charge radii (equation (3.13)), which is based on the rms radii, has been observed and is given by [7]

$$\Delta R_{00}(\%) = \frac{R_{00,approximated} - R_{00,rms}}{R_{00,rms}} \cdot 100 \tag{5.5}$$

The approximation for the nuclear charge radius (equation (3.14)) reproduces the nuclear charge radius, based on the rms radius, very well with an absolute deviation of 1% in the mean.

In figure 5.10 the nuclear charge radii of equations (3.13) and (3.14)) are compared.
In figure 5.11 the excitation functions for given rms radii (equation (3.14)) and for the approximation (equation 3.13) are compared to the experimental data. The neck formation and extra push corrected proximity potential was used for these excitation functions. As can be seen in figure 5.11 the excitation function based on rms radii mostly represents the the experimental data very well, whereas the excitation function based on the approximation (equation 3.13) agree much better with the experimental data for the reaction $'^{34}S + {}^{168}Er'$. As it can be observed a distinction in the excitation function is given by using either equation (3.14) or (3.13). But no statement can be made as no systematic deviation is observed.

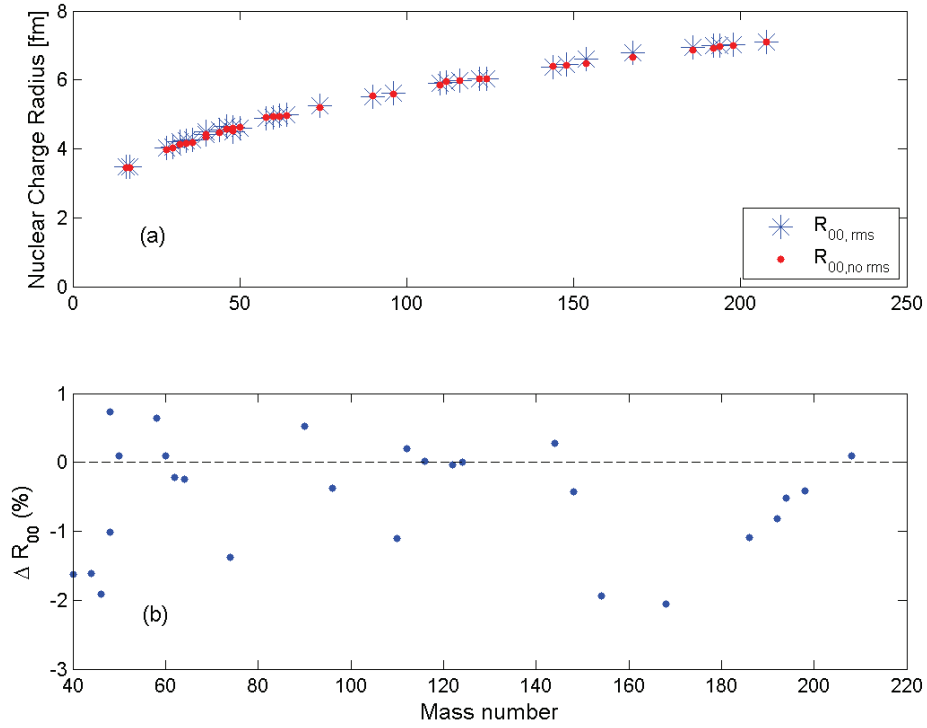

Figure 5.10: (**a**) Comparison between $R_{00,approximated}$ and $R_{00,rms}$. (**b**) Percentage difference ΔR_{00} in dependence on the mass number.

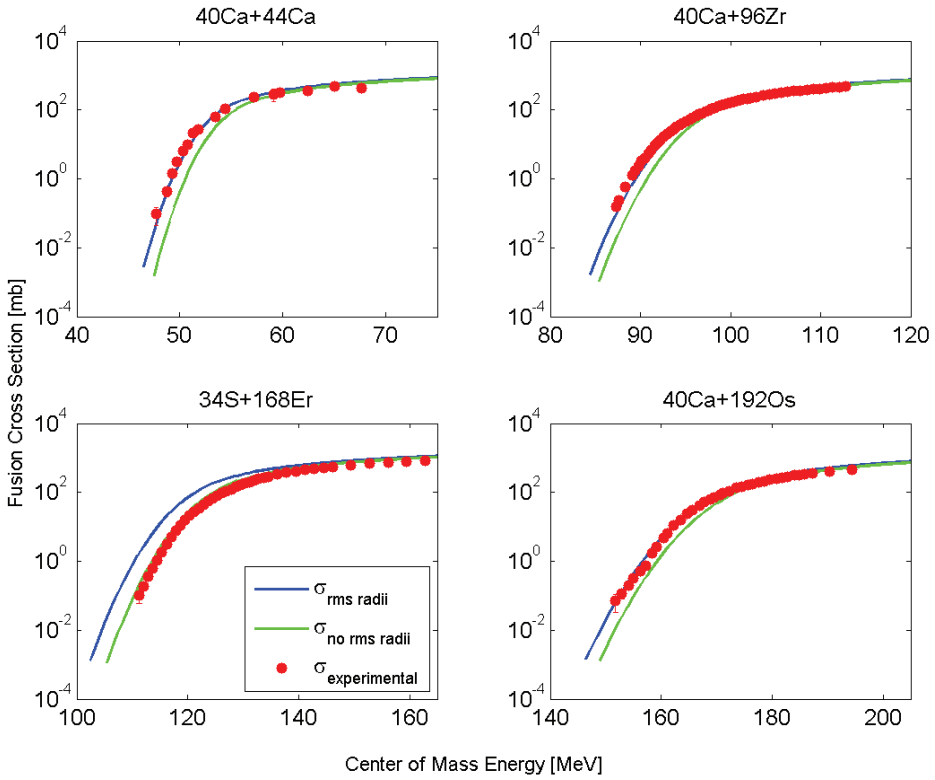

Figure 5.11: Comparison of excitation functions by using rms radii (equation (3.14)) or the approximation for no rms radii (equation (3.13)) for different reactions

5.5.3 Comparison of excitation functions for different width of the barrier height distribution

A comparison of the resultant excitation functions with the barrier heights calculated from the modified proximity potential and using theoretical and fitted values for width of the barrier height distribution w [4] has been made. As can be seen in figures (5.12-5.14) there are no systematic deviations for the two kinds of width of the barrier height distribution. For most reactions no significant deviation from the excitation functions, which were calculated by using w_{theo}, to excitation functions, determined by using w_{fit}, can be observed (e. g. figure (5.12)). For heavier reactions (figures (5.13-5.14)), a deviation of the two excitation functions is visible. But as already mentioned, there is no systematic deviation between the fitted and theoretical width of the barrier height distribution. While in figure (5.13), the excitation function of $w_{theo} = 4.27\ MeV$ reproduces the experimental data very well, the excitation function of $w_{fit} = 3.40\ MeV$ deviates from the experimental data for low energies. On the contrary, the excitation function of $w_{fit} = 4.18\ MeV$ does reproduce the experimental data in figure (5.14) very well, for which the excitation function of $w_{theo} = 5.46\ MeV$ does not provide good results.

In figures (5.12-5.14) $\sigma_{w,fit}$ represents the excitation function using the proximity potential modified by neck formation and extra push as well as the fitted width of the barrier height distribution w_{fit} [4]. $\sigma_{w,theo}$ represents the excitation function using the proximity potential modified by neck formation and extra push as well as the theoretically determined width of the barrier height distribution w_{theo} [4]. $\sigma_{woods-saxon}$ represents the excitation function using the fitted barrier height [4] as well as the fitted width of the barrier height distribution w_{fit} [4].

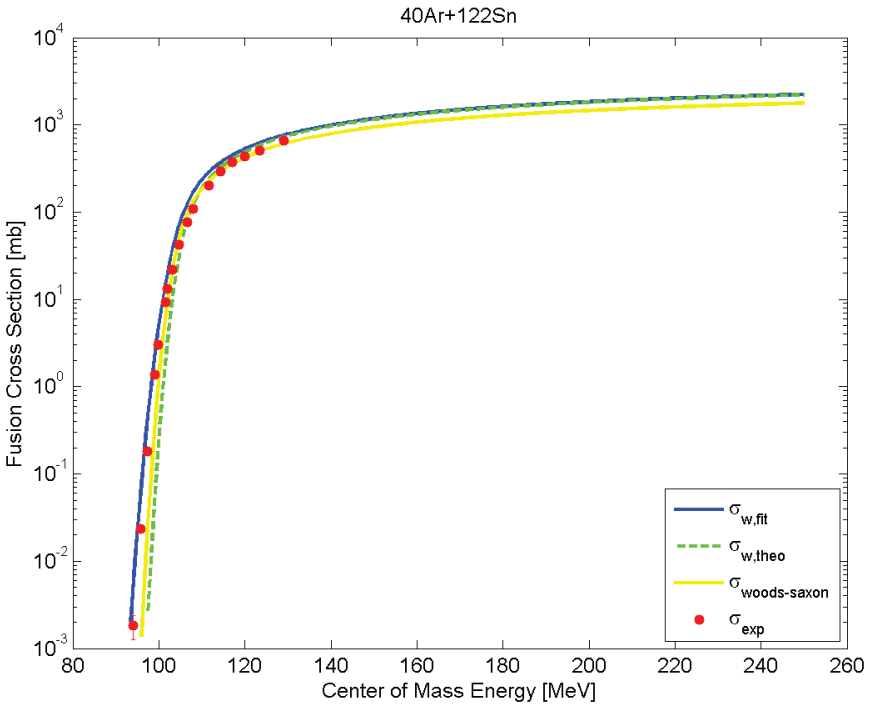

Figure 5.12: Excitation functions for the fitted width of the barrier height distribution w_{fit} and the theoretical width of the barrier height distribution w_{theo} in comparison to the excitation function from woods-saxon [4] and experimental data [22].

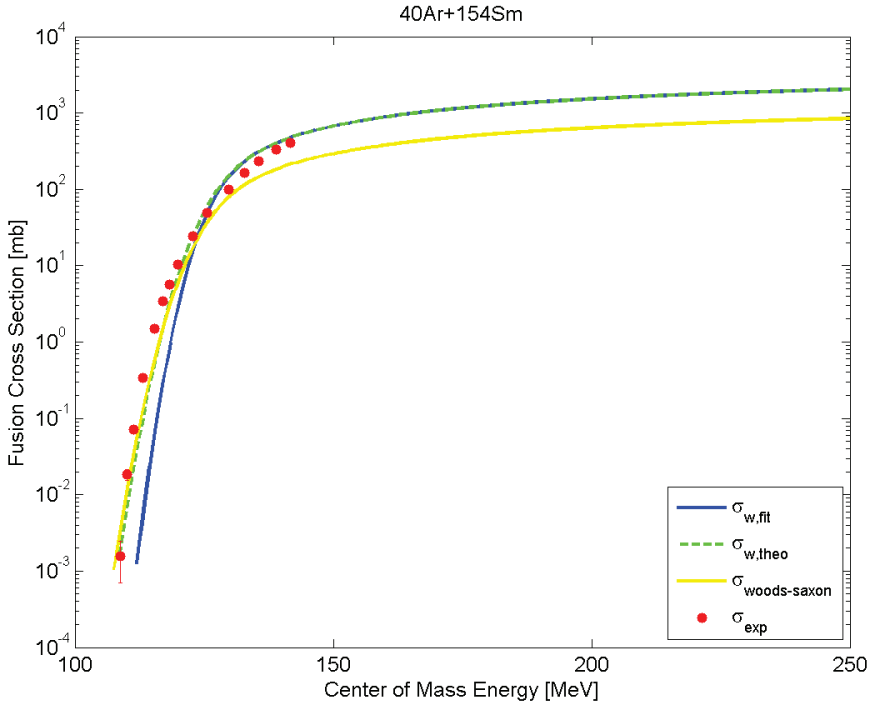

Figure 5.13: Excitation functions for the fitted width of the barrier height distribution w_{fit} and the theoretical width of the barrier height distribution w_{theo} in comparison to the excitation function from woods-saxon [4] and experimental data [22]. In this case, the nuclear charge radii have been calculated by equation (3.14).

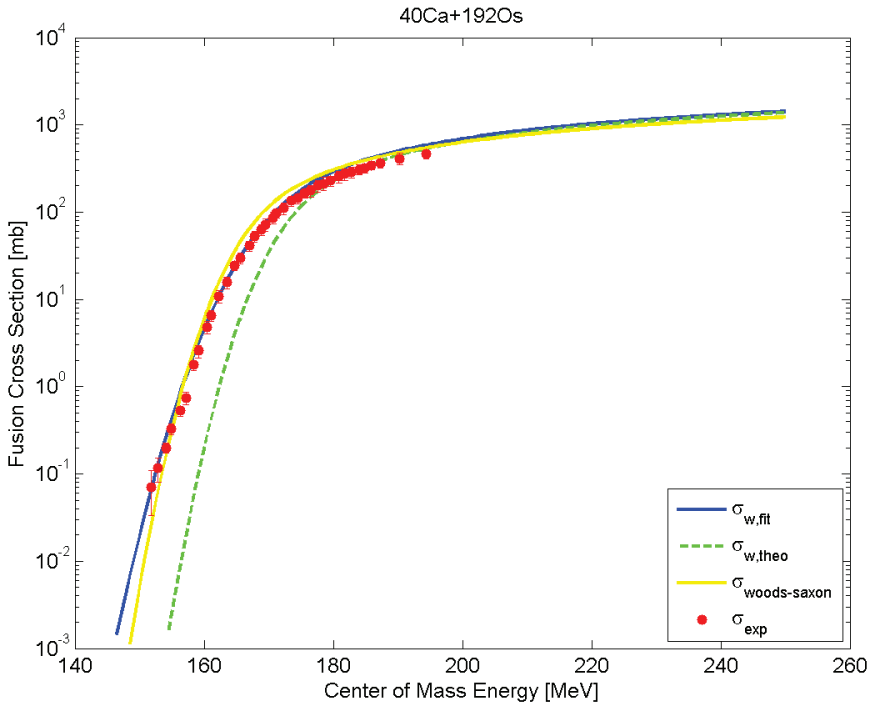

Figure 5.14: Excitation functions for the fitted width of the barrier height distribution w_{fit} and the theoretical width of the barrier height distribution w_{theo} in comparison to the excitation function from woods-saxon [4] and experimental data [21].

6 Conclusio

In this work, the fusion barrier heights and excitation functions for 48 measured fusion reactions have been studied. For the calculation of the fusion barrier heights, the proximity potential and modifications of it by neck formation and extra push were used. A comparison between these models (the original proximity potential, the proximity potential corrected by neck formation and the proximity potential corrected by neck formation and extra push) and the experimental data, reveal an improvement in the prediction of the excitation functions. Whereas for the original proximity potential, an overestimation of the experimental data has been observed, the neck formation lowered this deviation to acceptable results. But for the two heavy fusion systems ($z > 130$), discrepancies were still present. Because of a small number of heavy fusion systems no clear statement can be made but for the two analysed heavy fusion reactions, these discrepancies were reduced by applying the extra push. The advantage of this modified proximity model is the agreement of the results to the experimental data with an absolute mean deviation of $\overline{\triangle V} = 0.8155 \pm 0.0878\ MeV$ for all 48 fusion reactions. Furthermore no adaptation to experimental data is needed in this model. So this modified proximity model reproduces the experimental data with an acceptable accuracy without necessary alignments to measurements.

An analysis of the nuclear charge radius derived either by rms radii (equation (3.13)) or by an approximation (equation (3.14)), yield a change for the worse by using the approximation.

Last but not least, a comparison between excitation functions determined by either fitted width of the barrier height distribution w_{fit} or theoretically predicted width of the barrier height distribution w_{theo} has been made. In this analysis, no systematic deviation could be observed.

This simple model, for which no alignment to experimental data is necessary, produces almost as good results as the distributed barrier model with the woods-saxon potential [4] and is much simpler than the coupled channel calculation in use.

Acknowledgements

I would like to thank Professor Friedmann and Professor Hille for their excellent support through their expertise, without that this thesis would not have been possible. They advised and supervised me throughout the realization of this thesis. Their patience allowed me to finish this work alongside my other commitments.

I want to thank my parents, as they made it possible for me to accomplish academics studies in physics without any stress from their side, which made the duration of study for me an unforgettable time of my life. I am grateful for their generosity, their understanding and their confidence in me.

Furthermore, I want to thank Kieran Leschinski and Mag. Johannes Holztrattner for proof reading my thesis.

In the end, I would like to acknowledge my friend and colleague Alfons, who was a great support during this period. Without his optimism and his encouraging words, this thesis would have been a huge challenge for me.

Appendix

```
function proximity_potential_rms

clear all

%-------------------------------------------------------------------------
%Loading the Exel File
%-------------------------------------------------------------------------

[num,txt,name]=xlsread('K:\Diplom\Berechnung\Matlab\Berechnung nach Myers(Daten Matlab).xls');
[num1,txt1,name1]=xlsread('K:\Diplom\Berechnung\Matlab\Daten_Reaktionen.xls');

%-------------------------------------------------------------------------
%Declarations of variables
%-------------------------------------------------------------------------

e=sqrt((1.43996));
%[MeV fm]^(1/2), charge unit
hbarc=197.3269718;
%[MeV fm], reduced Planck constant multiplied by light speed [m/s], light
%speed
Z=nan(size(num,1),2);
%designs a matrix with two columns for the atomic number which adapts to
%the size of the input data
A=nan(size(num,1),2);
%mass number
rms=nan(size(num,1),2);
%[fm], rms charge radii  [10]
w=nan(size(num,1),1);
%[MeV], barrier height distribution (one column)  [4]
V0fit=nan(size(num,1),1);
%fitted barrier heights  [4]
R0fit=nan(size(num,1),1);
%effektive Radius [fm]
V0wilc=nan(size(num,1),1);
%derived by the model of K. Siwek-Wilczynska and J. Wilczynski  [4]
%(one column)
w_theo=nan(size(num,1),1);
%[MeV], theoretical barrier height distribution of K. Siwek-Wilczynska and
%J. Wilczynski  [4] (one column)

txt(1,:)=[];
%deletes the headline of the input file
txt(:,2:size(txt,2))=[];

pathname = {'K:\Diplom\Berechnung\Matlab\Plots\analysis\deviation\';...
    'K:\Diplom\Berechnung\Matlab\Plots\analysis\correlation\'};

pathname1 =  {'K:\Diplom\Berechnung\Matlab\Plots\potential\'};
```

```
pathname2 = {'K:\Diplom\Berechnung\Matlab\Plots\excitation_function\excitation_function\';
    'K:\Diplom\Berechnung\Matlab\Plots\excitation_function\wfit_vs_wtheo\'};
%defines the memory location

for i=1:size(Z,2)
    Z(:,i)=num(:,i);
    A(:,i)=num(:,i+2);
    rms(:,i)=num(:,i+4);
end
%fills the matrices with datas
w(:,1)=num(:,7);
V0fit(:,1)=num(:,8);
R0fit(:,1)=num(:,9);
V0wilc(:,1)=num(:,10);
%fills the matrices with datas
coulpara(:,1)=num(:,11);
%Coulomb Parameter
w_theo(:,1)=num(:,12);

%-------------------------------------------------------------------------
%Call functions
%-------------------------------------------------------------------------

[K, V0, R0, run, norms]=fusion_potential(Z,A,rms,e);
[Vneck, deltaVneck]=neck_potential(Z,A,V0);
[Vextrapush, deltaVextrapush]=extrapush(Z,A,e,hbarc,Vneck);
[run1, E]=excitation_function(w,V0,Vneck,Vextrapush,V0fit,A,V0wilc,w_theo,R0fit,R0);
[delta, ana]=analysis(Z, A, w, K, Vextrapush, R0, V0, V0fit, V0wilc, Vneck);
trend(V0, Vneck, Vextrapush, V0fit, V0wilc, coulpara);

run.X0=run1.X0;
run.Xneck=run1.Xneck;
run.Xextrapush=run1.Xextrapush;
run.X0fit=run1.X0fit;
run.Xwilc=run1.Xwilc;
run.Xw_theo=run1.Xw_theo;
%simplifies the code by adding two cell-arrays
run.sigma0=run1.sigma0;
run.sigmaneck=run1.sigmaneck;
run.sigmaextrapush=run1.sigmaextrapush;
run.sigmaV0fit=run1.sigmaV0fit;
run.sigmawilc=run1.sigmawilc;
run.sigmaw_theo=run1.sigmaw_theo;
run.sigmaexp=cell(size(Z,1),1);
run.sigmaexperror=cell(size(Z,1),1);
run.sigmaexpenergy=cell(size(Z,1),1);
clear run1; clear run2;
%deletes the cell-array run1 after beeing added to the cell-array run

for j=1:4:size(txt1,2)
    for i=1:size(txt,1)
        if strcmp(txt(i,1),txt1(2,j))==1
           %compares data in order to plot theoretical data of a reaction
           %against its experimental measured data
           expreactions(i,1)=1;
           run.sigmaexpenergy{i,1}=num1(:,j);
           run.sigmaexp{i,1}=num1(:,j+1);
           run.sigmaexperror{i,1}=num1(:,j+2);
```

```
            run.sigmaexpenergy{i,1}(isnan(run.sigmaexpenergy{i,1}))=[];
            run.sigmaexp{i,1}(isnan(run.sigmaexp{i,1}))=[];
            run.sigmaexperror{i,1}(isnan(run.sigmaexperror{i,1}))=0;
            x=size(run.sigmaexp{i,1},1);
            y=size(run.sigmaexperror{i,1},1);
            run.sigmaexperror{i,1}(x+1:y)=[];
        end
    end
end

xlswrite('norms',norms);

%calls the functions which include the plot commands
plotten(delta, txt, run, ana, E, V0, Vextrapush, V0fit, R0, expreactions,...
    pathname, pathname1, pathname2, coulpara, A, Z, rms);

end

function [K, V0, R0, run, norms]=fusion_potential(Z,A,rms,e)

%-------------------------------------------------------------------------
%Constants used for determination of the proximity potential  [1]
%-------------------------------------------------------------------------

Q=35.4;
%[MeV], neutron skin stiffnes coefficient
r0=1.14;
%[fm], constant radius
b=1;
%[fm], Süssman measure of the diffuseness of the nuclear surface
J=32.65;
%[MeV], symmetry energy coefficient
c1=0.757895;
%[MeV]

cn=[-0.1886; -0.2628; -0.15216; -0.04562; 0.069136; -0.011454];
%constants for calculation of the proximity potential

%-------------------------------------------------------------------------
%Declaration of variables
%-------------------------------------------------------------------------

R00=nan(size(Z,1),4);
%[fm], equivalent rms radii
I=nan(size(Z,1),2);
%asymmetry term
t=nan(size(Z,1),2);
%[fm], neutron skin
c=nan(size(Z,1),4);
%[fm], half density Radius
C12=nan(size(Z,1),6);
%[fm], matter radius/locate half density radii of matter distribution
a=nan(size(Z,1),1);
%[MeV], surface energy coefficient
gamma=nan(size(Z,1),1);
%[MeV fm^(-2)], mean surface tension coefficient
C=nan(size(Z,1),2);
%[fm], reduced radius
K=nan(size(Z,1),2);
```

```
%[MeV], strength factor
run.distance=cell(size(Z,1),2);
%creates a cell array which are arrays in each cell of the cell array; in
%this case there are as many cell arrays as the number of reactions; this
%cell array defines the run of the center seperation distance for each
%reaction
run.zeta=cell(size(Z,1),2);
%seperation distance
run.proxfac=cell(size(Z,1),2);
%defines the run for the proximity function used for the calculation for
%the Proximity potential
run.proxpot=cell(size(Z,1),2);
%[MeV], Proximity potential
run.coul=cell(size(Z,1),2);
%[MeV], Coulomb potential
run.interactpot=cell(size(Z,1),2);
%[MeV], nucleus-nucleus interaction potential
run.proxforce=cell(size(Z,1),2);
%Proximity force function
run.V0=cell(size(Z,1),2);
%[MeV fm^(-1)], run of the barrier height [MeV]
V0=nan(size(Z,1),2);
%[MeV], barrier height
R0=nan(size(Z,1),2);
%[fm], barrier height location
norms=nan(size(Z,1),1);

%-------------------------------------------------------------------------
%Calculation
%-------------------------------------------------------------------------

for q=1:2
    %q=1 no rms radii
    %q=2 rms radii are given

for i=1:size(Z,2)
    for j=1:size(Z,1)
        if q==1
            R00(j,i)=1.240*A(j,i)^(1/3)*(1+1.646/A(j,i)-0.191*(A(j,i)-...
                2*Z(j,i))/A(j,i));
        else
            R00(j,i+2)=sqrt(5/3)*rms(j,i);
            if isnan(R00(j,i+2))==1
                R00(j,i+2)=1.240*A(j,i)^(1/3)*(1+1.646/A(j,i)-0.191*(A(j,i)-...
                2*Z(j,i))/A(j,i));
                norms(j,1)=1;
            else
                norms(j,1)=0;
            end
        end
    end
end

for i=1:size(Z,2)
    for j=1:size(Z,1)
        I(j,i)=(A(j,i)-2*Z(j,i))/A(j,i);
        t(j,i)=(3/2)*r0*(J*I(j,i)-(1/12)*c1*Z(j,i)*A(j,i)^(-1/3))/...
            (Q+(9/4)*J*A(j,i)^(-1/3));
        if q==1
```

```
            c(j,i)=R00(j,i)*(1-(7/2)*(b^2/R00(j,i)^2)-(49/8)*(b^4/R00(j,i)^4));
            C12(j,i)=c(j,i)+(A(j,i)-Z(j,i))/A(j,i)*t(j,i);
        else
            c(j,i+2)=R00(j,i+2)*(1-(7/2)*(b^2/R00(j,i+2)^2)-(49/8)*(b^4/R00(j,i+2)^4));
            C12(j,i+3)=c(j,i+2)+(A(j,i)-Z(j,i))/A(j,i)*t(j,i);
        end
    end
end

if q==1
    m=0;
else
    m=3;
end

for i=1:size(Z,1)
    a(i,1)=18.36-Q*(t(i,1)^2+t(i,2)^2)/(2*r0^2);
    gamma(i,1)=a(i,1)/(4*pi*r0^2);
    C(i,q)=(C12(i,1+m)*C12(i,2+m))/(C12(i,1+m)+C12(i,2+m));
    K(i,q)=(b*a(i,1)*C(i,q))/r0^2;
    C12(i,3+m)=C12(i,1+m)+C12(i,2+m);
end

for j=1:size(C12,1)
    run.distance{j,q}(1,1)=C12(j,1+m)+C12(j,2+m);
    %defines the initial value of the center seperation distance
    for i=2:2000
        run.distance{j,q}(i,1)=run.distance{j,q}(i-1,1)+0.01;
    end
end

for j=1:size(C12,1)
    for i=1:size(run.distance{1,1},1)
        run.zeta{j,q}(i,1)=run.distance{j,q}(i,1)-C12(j,3+m);
    end
end

%-------------------------------------------------------------------------
%Calculation of the Proximity Potential
%-------------------------------------------------------------------------

for j=1:size(run.zeta,1)
    for i=1:size(run.zeta{1,1},1)
        if run.zeta{j,q}(i,1)>0 && run.zeta{j,q}(i,1)<2.5
            y=0;
            for n=1:size(cn,1)
                x=(cn(n,1)*(2.5-run.zeta{j,q}(i,1))^n)/n;
                y=y+x;
            end
            run.proxfac{j,q}(i,1)=-0.1353+y;
        elseif run.zeta{j,q}(i,1)>=2.5
            run.proxfac{j,q}(i,1)=-0.09551*exp((2.75-run.zeta{j,q}(i,1))/0.7176);
        end
    end
end

for j=1:size(run.zeta,1)
    for i=2:size(run.zeta{1,1},1)
        run.proxpot{j,q}(i,1)=K(j,q)*run.proxfac{j,q}(i,1);
```

```
    end
end

%-------------------------------------------------------------------------
%Calculation of the nucleus-nucleus interaction Potential
%-------------------------------------------------------------------------

for j=1:size(run.zeta,1)
    for i=2:size(run.zeta{1,1},1)
        run.coul{j,q}(i,1)=Z(j,1)*Z(j,2)*e^2/run.distance{j,q}(i,1);
        run.interactpot{j,q}(i,1)=run.coul{j,q}(i,1)+run.proxpot{j,q}(i,1);
    end
end

%-------------------------------------------------------------------------
%Calculation of the barrier height
%-------------------------------------------------------------------------

for j=1:size(run.zeta,1)
    for i=1:size(run.zeta{1,1},1)
        if run.zeta{j,q}(i,1)>0 && run.zeta{j,q}(i,1)<2.5
            y=0;
            for n=1:size(cn,1)
                x=(cn(n,1)*(2.5-run.zeta{j,q}(i,1))^(n-1));
                y=y+x;
            end
            run.proxforce{j,q}(i,1)=y;
        elseif run.zeta{j,q}(i,1)>=2.5
            run.proxforce{j,q}(i,1)=-0.1331*exp((2.75-run.zeta{j,q}(i,1))/0.7176);
        end
    end
end

for j=1:size(run.zeta,1)
    for i=2:size(run.zeta{1,1},1)
        run.V0{j,q}(i,1)=run.coul{j,q}(i,1)/run.distance{j,q}(i,1)+...
            run.proxforce{j,q}(i,1)*K(j,q)/b;
    end
end

%looks for the barrier height and its position
for j=1:size(run.distance,1)
    vorzeichen=sign(run.V0{j,q});
    maxima=find(diff(vorzeichen)>0);
    V0(j,q)=run.interactpot{j,q}(maxima,1);
    R0(j,q)=run.distance{j,q}(maxima,1);
end

end
end

function [Vneck, deltaVneck]=neck_potential(Z,A,V0)

%-------------------------------------------------------------------------
%Constants used for correction by the Neck potential  [2]
%-------------------------------------------------------------------------

%constants based on the parametrization of deltaVneck:
alpha=0.0016;
```

```
%[MeV]
beta=2.5;

%-------------------------------------------------------------------------
%Declaration of variables
%-------------------------------------------------------------------------

zeta=nan(size(Z,1),1);
%effective fissility
deltaVneck=nan(size(Z,1),1);
%difference gained by the Neck potential
Vneck=nan(size(Z,1),2);
%[MeV], critical value

%-------------------------------------------------------------------------
%Calculation
%-------------------------------------------------------------------------

for q=1:2
    for i=1:size(V0,1)
        zeta(i,1)=(4*Z(i,1)*Z(i,2))/(A(i,1)^(1/3)*A(i,2)^(1/3)*(A(i,1)^(1/3)+...
            A(i,2)^(1/3)));
        deltaVneck(i,1)=alpha*(zeta(i,1))^beta;
        Vneck(i,q)=V0(i,q)-deltaVneck(i,1);
    end
end

end

function [Vextrapush, deltaVextrapush]=extrapush(Z,A,e,hbarc,Vneck)

%-------------------------------------------------------------------------
%Constants used for correction by the Extra Push potential  [3]
%-------------------------------------------------------------------------

a=5;
%numerical constants
fissthr=26;
%threshold value for (Z^2/A)eff,thr
m=931;
%[MeV/c^2]

%-------------------------------------------------------------------------
%Declaration of variables
%-------------------------------------------------------------------------

K=nan(size(Z,1),1);
%factor used for the calculation for the correction of the barrier height
%by the Extra Push
fiss=nan(size(Z,1),1);
%fissility factor
Vextrapush=nan(size(Z,1),2);
%corrected form of the barrier height
deltaVextrapush=nan(size(Z,1),1);
%difference gained by the Neck potential

%-------------------------------------------------------------------------
%Calculation
%-------------------------------------------------------------------------
```

```
for q=1:2
    for i=1:size(Z,1)
        K(i,1)=((A(i,1)^(1/3)*A(i,2)^(1/3)*(A(i,1)^(1/3)+A(i,2)^(1/3))^(2))/...
            (A(i,1)+A(i,2)))*(32/2025)*((3/pi)^(2/3))*((e^2/(hbarc))^(2))*m*(a^(2));
        fiss(i,1)=(4*Z(i,1)*Z(i,2))/(A(i,1)^(1/3)*A(i,2)^(1/3)*(A(i,1)^(1/3)+...
            A(i,2)^(1/3)));
        if fiss(i,1)<=fissthr
            deltaVextrapush(i,1)=0;
        else
            deltaVextrapush(i,1)=K(i,1)*(fiss(i,1)-fissthr)^2;
        end
        Vextrapush(i,q)=Vneck(i,q)+deltaVextrapush(i,1);
    end
end

end

function [run1, E]=excitation_function(w,V0,Vneck,Vextrapush,V0fit,A,V0wilc,...
    w_theo,R0fit,R0)

%-------------------------------------------------------------------------
%Declaration of variables
%-------------------------------------------------------------------------

E=[40:0.5:250]';
%run for energy at a stepsize of 1
run1.X0=cell(size(w,1),2);
run1.Xneck=cell(size(w,1),2);
run1.Xextrapush=cell(size(w,1),2);
run1.X0fit=cell(size(w,1),1);
%X_i is the variable used in the formula for the fusion cross section
run1.sigma0=cell(size(w,1),2);
%run of the fusion cross section for the uncorrected proximity model
run1.sigmaneck=cell(size(w,1),2);
%run of the fusion cross section for the by neck formation corrected
%proximity model
run1.sigmaextrapush=cell(size(w,1),2);
%run of the fusion cross section for the by neck formation and extra push
%corrected proximity model
run1.sigmaV0fit=cell(size(w,1),1);
%Rsigma=nan(size(A,1),1);
%is the sum of the radii of the two nuclei

%-------------------------------------------------------------------------
%Calculation
%-------------------------------------------------------------------------

for q=1:2
%     for j=1:size(A,1)
%         Rsigma(j,1)=1.27*(A(j,1)^(1/3)+A(j,2)^(1/3));
%     end

    %calculates the excitation function for each model
    for i=1:size(w,1)
        for j=1:size(E,1)
            run1.X0{i,q}(j,1)=(E(j,1)-V0(i,q))/(sqrt(2)*w(i,1));
            run1.sigma0{i,q}(j,1)=pi*R0(i,1)^2*w(i,1)*(run1.X0{i,q}(j,1)*sqrt(pi)...
                *(1+erf(run1.X0{i,q}(j,1)))+exp(-run1.X0{i,q}(j,1)^2))/(E(j,1)*sqrt(2*pi));
```

```
            %-------------------------------------------------------------------
            run1.Xneck{i,q}(j,1)=(E(j,1)-Vneck(i,q))/(sqrt(2)*w(i,1));
            run1.sigmaneck{i,q}(j,1)=pi*R0(i,1)^2*w(i,1)*(run1.Xneck{i,q}(j,1)*...
                sqrt(pi)*(1+erf(run1.Xneck{i,q}(j,1)))+exp(-run1.Xneck{i,q}(j,1)^2))...
                /(E(j,1)*sqrt(2*pi));
            %-------------------------------------------------------------------
            run1.Xextrapush{i,q}(j,1)=(E(j,1)-Vextrapush(i,q))/(sqrt(2)*w(i,1));
            run1.sigmaextrapush{i,q}(j,1)=pi*R0(i,1)^2*w(i,1)*(run1.Xextrapush{i,q}...
                (j,1)*sqrt(pi)*(1+erf(run1.Xextrapush{i,q}(j,1)))+exp(-run1.Xextrapush...
                {i,q}(j,1)^2))/(E(j,1)*sqrt(2*pi));
            %-------------------------------------------------------------------
            run1.X0fit{i,1}(j,1)=(E(j,1)-V0fit(i,1))/(sqrt(2)*w(i,1));
            run1.sigmaV0fit{i,1}(j,1)=pi*R0(i,1)^2*w(i,1)*(run1.X0fit{i,1}(j,1)*...
                sqrt(pi)*(1+erf(run1.X0fit{i,1}(j,1)))+exp(-run1.X0fit{i,1}(j,1)^2))...
                /(E(j,1)*sqrt(2*pi));
            %-------------------------------------------------------------------
            run1.Xwilc{i,q}(j,1)=(E(j,1)-V0wilc(i,1))/(sqrt(2)*w_theo(i,1));
            run1.sigmawilc{i,q}(j,1)=pi*R0fit(i,1)^2*w_theo(i,1)*(run1.Xwilc{i,q}(j,1)*...
                sqrt(pi)*(1+erf(run1.Xwilc{i,q}(j,1)))+exp(-run1.Xwilc{i,q}(j,1)^2))/...
                (E(j,1)*sqrt(2*pi));
            %-------------------------------------------------------------------
            run1.Xw_theo{i,q}(j,1)=(E(j,1)-Vextrapush(i,1))/(sqrt(2)*w_theo(i,1));
            run1.sigmaw_theo{i,q}(j,1)=pi*R0(i,1)^2*w_theo(i,1)*(run1.Xw_theo{i,q}(j,1)*...
                sqrt(pi)*(1+erf(run1.Xw_theo{i,q}(j,1)))+exp(-run1.Xw_theo{i,q}(j,1)^2))/...
                (E(j,1)*sqrt(2*pi));
        end
    end
end

end

function [delta, ana]=analysis(Z, A, w, K, Vextrapush, R0, V0, V0fit, V0wilc, ...
    Vneck)

%-------------------------------------------------------------------------
%Declaration of variables
%-------------------------------------------------------------------------

ana.fissility=nan(size(Z,1),1);
ana.coulomb=nan(size(Z,1),1);
N=nan(size(Z,1),2);
delta.V0=nan(size(Z,1)+1,2);
delta.V1=nan(size(Z,1)+1,2);
delta.V2=nan(size(Z,1)+1,2);
delta.V3=nan(size(Z,1)+1,2);
delta.V01=nan(size(Z,1),2);
delta.V11=nan(size(Z,1),2);
delta.V21=nan(size(Z,1),2);
delta.V31=nan(size(Z,1),2);

%-------------------------------------------------------------------------
%Calculations
%-------------------------------------------------------------------------

for i=1:size(Z,1)
    N(i,1)=A(i,1)-Z(i,1);
    N(i,2)=A(i,2)-Z(i,2);
    ana.fissility(i,1)=(4*Z(i,1)*Z(i,2))/((A(i,1)^(1/3))*(A(i,2)^(1/3))*...
        ((A(i,1)^(1/3))+A(i,2)^(1/3)));
```

```
    ana.coulomb(i,1)=(Z(i,1)*Z(i,2))/((A(i,1)^(1/3))+(A(i,2)^(1/3)));
end

for q=1:2
    for i=1:size(V0fit,1)
        delta.V0(i,q)=(V0(i,q)-V0fit(i,1));
        delta.V1(i,q)=(Vneck(i,q)-V0fit(i,1));
        delta.V2(i,q)=(Vextrapush(i,q)-V0fit(i,1));
        delta.V3(i,q)=(V0wilc(i,1)-V0fit(i,1));
    end

%-------------------------------------------------------------------------
%Statistics
%-------------------------------------------------------------------------

mittel(1,q)=mean(delta.V0(:,q));
stand(1,q)=std(delta.V0(:,q));
standstand(1,q)=stand(:,1)/sqrt(size(Z,1)-1);

delta.V01(:,q)=abs(delta.V0(1:size(delta.V0,1)-1,q));
delta.V11(:,q)=abs(delta.V1(1:size(delta.V1,1)-1,q));
delta.V21(:,q)=abs(delta.V2(1:size(delta.V2,1)-1,q));
delta.V31(:,q)=abs(delta.V3(1:size(delta.V3,1)-1,q));

delta.V0(size(delta.V0,1),q)=mean(delta.V01(:,q));
delta.V1(size(delta.V1,1),q)=mean(delta.V11(:,q));
delta.V2(size(delta.V2,1),q)=mean(delta.V21(:,q));
delta.V3(size(delta.V3,1),q)=mean(delta.V31(:,q));

end
end

function trend(V0, Vneck, Vextrapush, V0fit, V0wilc, coulpara)

%-------------------------------------------------------------------------
%%analyses the deviation of the determined barrier height datas from the
%fitted measured values  [4]:
%-------------------------------------------------------------------------

calculation=nan(size(V0,1),4);
calc=nan(size(V0,1),4);
result=nan(16,5);
deltaVprox=nan(size(V0,1)+1,2);
deltaVneck=nan(size(V0,1)+1,2);
deltaVextra=nan(size(V0,1)+1,2);
deltaVwoods=nan(size(V0,1)+1,2);
calc=nan(size(V0,1),8);

for q=1:2
    calculation(:,1)=abs(V0(:,q)-V0fit);
    calculation(:,2)=abs(Vneck(:,q)-V0fit);
    calculation(:,3)=abs(Vextrapush(:,q)-V0fit);
    calculation(:,4)=abs(V0wilc-V0fit);

    %result(1,2)='Proximity Potential';
    %result(1,3)='Neck Formation';
    %result(1,4)='Extrapush';
    %result(1,5)='Wilcinzky';
    %result(2,1)='z<70';
```

```
    %result(6,1)='70<z<130';
    %result(10,1)='z<130';
    %result(14,1)='all';

    x=find(coulpara<=70);
    y=find(coulpara<=130);
    z=find(coulpara>130);

    calc(:,q)=V0(:,q)-V0fit;
    calc(:,q+2)=Vneck(:,q)-V0fit;
    calc(:,q+4)=Vextrapush(:,q)-V0fit;
    calc(:,q+6)=V0wilc-V0fit;
    for i=1:size(V0,1)
        deltaVprox(i,q)=(calc(i,q)/V0fit(i,1))*100;
        deltaVneck(i,q)=(calc(i,q+2)/V0fit(i,1))*100;
        deltaVextra(i,q)=(calc(i,q+4)/V0fit(i,1))*100;
        deltaVwoods(i,q)=(calc(i,q+6)/V0fit(i,1))*100;
    end

    deltaVprox(size(deltaVprox,1),q)=0;
    deltaVneck(size(deltaVneck,1),q)=0;
    deltaVextra(size(deltaVextra,1),q)=0;
    deltaVwoods(size(deltaVwoods,1),q)=0;

    for i=1:size(V0,1)
        deltaVprox(size(deltaVprox,1),q)=deltaVprox(size(deltaVprox,1),q)+abs(deltaVprox(i,q));
        deltaVneck(size(deltaVneck,1),q)=deltaVneck(size(deltaVneck,1),q)+abs(deltaVneck(i,q));
        deltaVextra(size(deltaVextra,1),q)=deltaVextra(size(deltaVextra,1),q)+abs(deltaVextra(i,q));
        deltaVwoods(size(deltaVwoods,1),q)=deltaVwoods(size(deltaVwoods,1),q)+abs(deltaVwoods(i,q));
    end

    deltaVprox(size(deltaVprox,1),q)=deltaVprox(size(deltaVprox,1),q)/size(V0,1);
    deltaVneck(size(deltaVneck,1),q)=deltaVneck(size(deltaVneck,1),q)/size(V0,1);
    deltaVextra(size(deltaVextra,1),q)=deltaVextra(size(deltaVextra,1),q)/size(V0,1);
    deltaVwoods(size(deltaVwoods,1),q)=deltaVwoods(size(deltaVwoods,1),q)/size(V0,1);

    for i=1:4
        result(2,i+1)=mean(calculation(1:max(x),i));
        result(6,i+1)=mean(calculation(max(x):max(y),i));
        result(10,i+1)=mean(calculation(min(z):max(z),i));
        result(14,i+1)=mean(calculation(:,i));

        result(3,i+1)=std(calculation(1:max(x),i));
        result(7,i+1)=std(calculation(max(x):max(y),i));
        result(11,i+1)=std(calculation(min(z):max(z),i));
        result(15,i+1)=std(calculation(:,i));

        result(4,i+1)=result(3,i+1)/sqrt(size(calculation(1:max(x),1),1));
        result(8,i+1)=result(7,i+1)/sqrt(size(calculation(max(x):max(y),1),1));
        result(12,i+1)=result(11,i+1)/sqrt(size(calculation(min(z):max(z),1),1));
        result(16,i+1)=result(15,i+1)/sqrt(size(calculation,1));
    end

    if q==1
        xlswrite('normsdaten', result);
    else
        xlswrite('daten', result);
    end
end
```

```
end


function plotten(delta, txt, run, ana, E, V0, Vextrapush, V0fit, R0, expreactions,...
    pathname, pathname1, pathname2, coulpara, A, Z, rms)

for q=1:2

%-------------------------------------------------------------------------
%Plot nucleus-nucleus interaction potential
%-------------------------------------------------------------------------

for j=1:size(run.distance,1)
    h=figure('visible','off');
    plot(run.distance{j,q}(2:size(run.interactpot{j,q},1)),...
        run.interactpot{j,q}(2:size(run.interactpot{j,q},1)),'LineWidth',1.5);
    hold on
    a=get(gca,'XTickLabel');
    b=get(gca,'YTickLabel');
    a=str2num(a);
    b=str2num(b);
    x=find(R0(j,q)>a(:,1));
    y=find(V0(j,q)>b(:,1));
    c=(x:R0(j,q))';
    d=ones(size(c,1))*V0(j,q);
    plot(c,d,'-.','Color','k');
    e=(y:V0(j,q))';
    f=ones(size(e,1))*R0(j,q);
    plot(f,e,'-.','Color','k');
    plot(R0(j,q),V0(j,q),'*','MarkerSize',12);
    text(1,V0(j,q)+1,'V0','FontSize',12);
    text(R0(j,q),2,'R0','FontSize',12);
    ylim([0 max(b)+10]);
    ylabel('Nucleus-Nucleus Interaction Potential [MeV]','FontSize',12);
    xlabel('Center seperation distance [fm]','FontSize',12);
    title(txt(j,1),'FontSize',12);
    set(gca,'FontSize',12);
    if q==1
        saveas(gca, [pathname1{1,1} 'potential_norms_' num2str(j) '.png']);
    elseif q==2
        saveas(gca, [pathname1{1,1} 'potential_' num2str(j) '.png']);
    end
    close
end

%-------------------------------------------------------------------------
%excitation_function
%-------------------------------------------------------------------------

for j=1:size(run.sigmawilc,1)
    run.sigmawilc{j,q}=run.sigmawilc{j,q}*10;
    run.sigma0{j,q}=run.sigma0{j,q}*10;
    run.sigmaextrapush{j,q}=run.sigmaextrapush{j,q}*10;
    run.sigmaneck{j,q}=run.sigmaneck{j,q}*10;
    h=figure('visible','off');
    v=find(E<=170);
    w=find(run.sigma0{j,q}>0.001);
    x=find(run.sigmawilc{j,q}>0.001);
```

```
    y=find(run.sigmaextrapush{j,q}>0.001);
    z=find(run.sigmaneck{j,q}>0.001);
    if coulpara(j,1) <= 120
        plot(E(w:max(v),1),run.sigma0{j,q}(w:max(v),1),'-.','LineWidth',2.2);
        hold on
        plot(E(z:max(v),1),run.sigmaneck{j,q}(z:max(v),1),'--','LineWidth',2.2);
        plot(E(y:max(v),1),run.sigmaextrapush{j,q}(y:max(v),1),'LineWidth',2);
        plot(E(x:max(v),1),run.sigmawilc{j,q}(x:max(v),1),'Color','g','LineWidth',2.2);
        errorbar(run.sigmaexpenergy{j,1},run.sigmaexp{j,1},run.sigmaexperror{j,1},'.','Color',...
            'r','MarkerSize', 18);
        set(gca,'FontSize',12,'yscale','log');
        ylabel('Fusion Cross Section [mb]','FontSize',12);
        xlabel('Center of Mass Energy [MeV]','FontSize',12);
        legend('{\sigma}_{proximity potential}','{\sigma}_{neck formation}',...
            '{\sigma}_{extra push}','{\sigma}_{woods-saxon}','{\sigma}_{experimental}',4);
        title(txt(j,1),'FontSize',12);
        if q==1
           saveas(gca, [pathname2{1,1} 'excitationfct_prox_norms_' num2str(j) '.png']);
        elseif q==2
           saveas(gca, [pathname2{1,1} 'excitationfct_prox_' num2str(j) '.png']);
        end
        hold off
        close
    else
        plot(E(w:size(run.sigma0{j,q},1),1),run.sigma0{j,q}(w:size(run.sigma0{j,q},1)),'-.',...
            'LineWidth',1.8);
        hold on
        plot(E(z:size(run.sigmaneck{j,q},1),1),run.sigmaneck{j,q}(z:size(run.sigmaneck{j,q},1)),...
            '--','LineWidth',1.5);
        plot(E(y:size(run.sigmaextrapush{j,q},1),1),run.sigmaextrapush{j,q}...
            (y:size(run.sigmaextrapush{j,q},1)),'LineWidth',1.5);
        plot(E(x:size(run.sigmawilc{j,q},1),1),run.sigmawilc{j,q}(x:size(run.sigmawilc{j,q},1)),...
            'Color','g','LineWidth',1.5);
        errorbar(run.sigmaexpenergy{j,1},run.sigmaexp{j,1},run.sigmaexperror{j,1},'.','Color',...
            'r','MarkerSize', 18);
        set(gca,'FontSize',12,'yscale','log');
        ylabel('Fusion Cross Section [mb]','FontSize',12);
        xlabel('Center of Mass Energy [MeV]','FontSize',12);
        legend('{\sigma}_{proximity potential}','{\sigma}_{neck formation}',...
            '{\sigma}_{extra push}','{\sigma}_{woods-saxon}','{\sigma}_{experimental}',4);
        title(txt(j,1),'FontSize',12);
        if q==1
           saveas(gca, [pathname2{1,1} 'excitationfct_prox_norms_' num2str(j) '.png']);
        elseif q==2
           saveas(gca, [pathname2{1,1} 'excitationfct_prox_' num2str(j) '.png']);
        end
        hold off
        close
    end
end

%-------------------------------------------------------------------------
%w_fit vs w_theo
%-------------------------------------------------------------------------

for j=1:size(run.sigmaextrapush,1)
    run.sigmaw_theo{j,q}=run.sigmaw_theo{j,q}*10;
    h=figure('visible','off');
    x=find(run.sigmaw_theo{j,q}>0.001);
```

```
    y=find(run.sigmaextrapush{j,q}>0.001);
    z=find(run.sigmawilc{j,q}>0.001);
    plot(E(y:size(run.sigmaextrapush{j,q},1),1),run.sigmaextrapush{j,q}...
        (y:size(run.sigmaextrapush{j,q},1)),'LineWidth',2.2);
    hold on
    plot(E(x:size(run.sigmaw_theo{j,q},1),1),run.sigmaw_theo{j,q}...
        (x:size(run.sigmaw_theo{j,q},1)),'--','Color','g','LineWidth',2.2);
    plot(E(z:size(run.sigmawilc{j,q},1),1),run.sigmawilc{j,q}...
        (z:size(run.sigmawilc{j,q},1)),'Color','y','LineWidth',2.2);
    errorbar(run.sigmaexpenergy{j,1},run.sigmaexp{j,1},run.sigmaexperror{j,1},...
        '.','Color','r','MarkerSize', 18);
    set(gca,'FontSize',12,'yscale','log');
    ylabel('Fusion Cross Section [mb]','FontSize',12);
    xlabel('Center of Mass Energy [MeV]','FontSize',12);
    legend('{\sigma}_{w,fit}','{\sigma}_{w,theo}','{\sigma}_{woods-saxon}',...
        '{\sigma}_{exp}',4);
    title(txt(j,1),'FontSize',12);
    if q==1
       saveas(gca, [pathname2{2,1} 'w_against_w_norms_' num2str(j) '.png']);
    elseif q==2
       saveas(gca, [pathname2{2,1} 'w_against_w_' num2str(j) '.png']);
    end
    hold off
    close
end

%-------------------------------------------------------------------------
%Correlation
%-------------------------------------------------------------------------
h=figure('visible','off');
plot(ana.fissility,delta.V2(1:size(delta.V2,1)-1,q),'.','MarkerSize', 12);
set(gca,'FontSize',12);
a=get(gca,'XTickLabel');
a=str2num(a);
hold on
c=(min(a):max(a))';
d=zeros(size(c,1),1);
plot(c,d,'--','Color','k');
ylabel('{V}_{i}-{V}_{fit} [MeV]');
xlabel('Fissility');
if q==1
    saveas(gca, [pathname{2,1} 'correlation_norms.png']);
elseif q==2
    saveas(gca, [pathname{2,1} 'correlation.png']);
end
close
end

%-------------------------------------------------------------------------
%Subplot 4
%-------------------------------------------------------------------------

h=figure('visible','off');

w1=find(run.sigmaextrapush{9,1}>0.001);
w2=find(run.sigmaextrapush{9,2}>0.001);
x1=find(run.sigmaextrapush{32,1}>0.001);
x2=find(run.sigmaextrapush{32,2}>0.001);
y1=find(run.sigmaextrapush{43,1}>0.001);
```

```
y2=find(run.sigmaextrapush{43,2}>0.001);
z1=find(run.sigmaextrapush{47,1}>0.001);
z2=find(run.sigmaextrapush{47,2}>0.001);

subplot(2,2,1); plot(E(w2:size(run.sigmaextrapush{9,2},1),1),run.sigmaextrapush{9,2}...
       (w2:size(run.sigmaextrapush{9,2},1)),'LineWidth',1.5);
hold on
subplot(2,2,1); plot(E(w1:size(run.sigmaextrapush{9,1},1),1),run.sigmaextrapush{9,1}...
       (w1:size(run.sigmaextrapush{9,1},1)),'Color','g','LineWidth',1.5);
subplot(2,2,1); errorbar(run.sigmaexpenergy{9,1},run.sigmaexp{9,1},run.sigmaexperror{9,1},...
        '.','Color','r','MarkerSize', 18);
xlim([40 75]);
set(gca,'FontSize',12,'yscale','log');
title(txt(9,1),'FontSize',12);

subplot(2,2,2); plot(E(x2:size(run.sigmaextrapush{32,2},1),1),run.sigmaextrapush{32,2}...
       (x2:size(run.sigmaextrapush{32,2},1)),'LineWidth',1.5);
hold on
subplot(2,2,2); plot(E(x1:size(run.sigmaextrapush{32,1},1),1),run.sigmaextrapush{32,1}...
       (x1:size(run.sigmaextrapush{32,1},1)),'Color','g','LineWidth',1.5);
subplot(2,2,2); errorbar(run.sigmaexpenergy{32,1},run.sigmaexp{32,1},run.sigmaexperror{32,1},...
        '.','Color','r','MarkerSize', 18);
xlim([80 120]);
set(gca,'FontSize',12,'yscale','log');
title(txt(32,1),'FontSize',12);

subplot(2,2,3); plot(E(y2:size(run.sigmaextrapush{43,2},1),1),run.sigmaextrapush{43,2}...
       (y2:size(run.sigmaextrapush{43,2},1)),'LineWidth',1.5);
hold on
subplot(2,2,3); plot(E(y1:size(run.sigmaextrapush{43,1},1),1),run.sigmaextrapush{43,1}...
       (y1:size(run.sigmaextrapush{43,1},1)),'Color','g','LineWidth',1.5);
subplot(2,2,3); errorbar(run.sigmaexpenergy{43,1},run.sigmaexp{43,1},run.sigmaexperror{43,1},...
        '.','Color','r','MarkerSize', 18);
legend('{\sigma}_{rms radii}', '{\sigma}_{no rms radii}','{\sigma}_{experimental}',4);
xlim([100 165]);
set(gca,'FontSize',12,'yscale','log');
title(txt(43,1),'FontSize',12);

subplot(2,2,4); plot(E(z2:size(run.sigmaextrapush{47,2},1),1),run.sigmaextrapush{47,2}...
       (z2:size(run.sigmaextrapush{47,2},1)),'LineWidth',1.5);
hold on
subplot(2,2,4); plot(E(z1:size(run.sigmaextrapush{47,1},1),1),run.sigmaextrapush{47,1}...
       (z1:size(run.sigmaextrapush{47,1},1)),'Color','g','LineWidth',1.5);
subplot(2,2,4); errorbar(run.sigmaexpenergy{47,1},run.sigmaexp{47,1},run.sigmaexperror{47,1},...
        '.','Color','r','MarkerSize', 18);
xlim([140 205]);
set(gca,'FontSize',12,'yscale','log');
title(txt(47,1),'FontSize',12);

[ax,h]=suplabel('Center of Mass Energy [MeV]','x',[.08 .08 .84 .84]);
hold on
[ax,h]=suplabel('Fusion Cross Section [mb]','y',[.12 .12 .74 .74]);

saveas(gca, [pathname{1,1} 'excitation_rms_norms.png']);
close

%-------------------------------------------------------------------------
%Deviation
%-------------------------------------------------------------------------
```

```
h=figure('visible','off');
subplot(4,1,1); plot(ana.coulomb, delta.V0(1:size(delta.V0,1)-1,2),'.','MarkerSize', 9);
a=get(gca,'XTickLabel');
a=str2num(a);
hold on
c=(min(a):max(a))';
d=zeros(size(c,1),1);
subplot(4,1,1); plot(c, d,'--','Color','k');
ylim([-4 11]);
title('Proximity Potential');

subplot(4,1,2); plot(ana.coulomb, delta.V1(1:size(delta.V1,1)-1,2),'.','MarkerSize', 9);
hold on
subplot(4,1,2); plot(c, d,'--','Color','k');
ylim([-10 5]);
title('Proximity Potential corrected by Neck Formation');

subplot(4,1,3); plot(ana.coulomb, delta.V2(1:size(delta.V2,1)-1,2),'.','MarkerSize', 9);
hold on
subplot(4,1,3); plot(c, d,'--','Color','k');
ylim([-5 5]);
title('Proximity Potential corrected by Neck Formation and by Extra Push');

subplot(4,1,4); plot(ana.coulomb, delta.V3(1:size(delta.V3,1)-1,2),'.','MarkerSize', 9);
title('Woods-Saxon Potential');
hold on
subplot(4,1,4); plot(c, d,'--','Color','k');
ylim([-5 5]);

xlabel('z');
hold on
[ax,h]=suplabel('{V}_{theo} - {V}_{fit} [MeV]','y',[.12 .12 .74 .74]);
%link(http://www.mathworks.com/matlabcentral/fileexchange/7772-suplabel,23.
%12.2012, 11:00)
saveas(gca, [pathname{1,1} 'deviation.png']);
close

%-------------------------------------------------------------------------
%pot_vs_pot_rm
%-------------------------------------------------------------------------

h=figure('visible','off');
subplot(3,1,1); plot(ana.coulomb, delta.V0(1:size(delta.V0,1)-1,2),...
    '.','MarkerSize', 9);
a=get(gca,'XTickLabel');
a=str2num(a);
hold on
subplot(3,1,1); plot(ana.coulomb, delta.V0(1:size(delta.V0,1)-1,1),...
    '.','Color','r','MarkerSize', 9);
c=(min(a):max(a))';
d=zeros(size(c,1),1);
subplot(3,1,1); plot(c, d,'--','Color','k');
ylim([-4 11]);
legend('rms radii', 'no rms radii');
title('Proximity Potential');

subplot(3,1,2); plot(ana.coulomb, delta.V1(1:size(delta.V1,1)-1,2),...
    '.','MarkerSize', 9);
```

```
hold on
subplot(3,1,2); plot(ana.coulomb, delta.V1(1:size(delta.V1,1)-1,1),...
    '.','Color','r','MarkerSize', 9);
subplot(3,1,2); plot(c, d,'--','Color','k');
ylim([-10 5]);
title('Proximity Potential corrected by Neck Formation');

subplot(3,1,3); plot(ana.coulomb, delta.V2(1:size(delta.V2,1)-1,2),...
    '.','MarkerSize', 9);
hold on
subplot(3,1,3); plot(ana.coulomb, delta.V2(1:size(delta.V2,1)-1,1),...
    '.','Color','r','MarkerSize', 9);
subplot(3,1,3); plot(c, d,'--','Color','k');
ylim([-5 5]);
title('Proximity Potential corrected by Neck Formation and by Extra Push');

xlabel('z');
hold on
[ax,h]=suplabel('{V}_{theo} - {V}_{fit} [MeV]','y',[.12 .12 .74 .74]);
%link(http://www.mathworks.com/matlabcentral/fileexchange/7772-suplabel,23.
%12.2012, 11:00)
saveas(gca,[pathname{1,1} 'pot_vs_pot_rms.png']);
close

%-------------------------------------------------------------------------
%R00 vs rms
%-------------------------------------------------------------------------

for i=1:size(Z,2)
    for j=1:size(Z,1)
        R00(j,i)=1.240*A(j,i)^(1/3)*(1+1.646/A(j,i)-0.191*(A(j,i)-...
                2*Z(j,i))/A(j,i));
        R00(j,i+2)=sqrt(5/3)*rms(j,i);
        deltaR00(j,i)=(R00(j,i)-R00(j,i+2))/R00(j,i+2)*100;
    end
end

f1=0;
for i=1:size(deltaR00,1)
    f=abs(deltaR00(i,1))+abs(deltaR00(i,2));
    f1=f1+f;
end

mittelwert=f1/(2*size(deltaR00,1));

h=figure('visible','off');
hold on
for i=1:size(A,2)
        subplot(2,1,1); plot(A(:,i),R00(:,i+2),'*','MarkerSize', 13);
        hold on
        subplot(2,1,1); plot(A(:,i),R00(:,i),'.','Color','r','MarkerSize', 12);
        hold on
        subplot(2,1,2); plot(A(:,i),deltaR00(:,i),'.','MarkerSize', 12);
end
hold on
a=get(gca,'XTickLabel');
a=str2num(a);
c=(min(a):max(a))';
d=zeros(size(c,1),1);
```

```
subplot(2,1,1); plot(c,d,'--','Color','k');
hold on
ylabel('Nuclear Charge Radius [fm]','FontSize',12);
legend('{R}_{00, rms}','{R}_{00,no rms}',4);
text(20,1.5,'(a)','FontSize',12);
subplot(2,1,2); plot(c,d,'--','Color','k');
hold on
ylabel('{\Delta R}_{00} (%)','FontSize',12);
text(55,-2.2,'(b)','FontSize',12);

xlabel('Mass number','FontSize',12);

set(gca,'box','on');
saveas(gca, [pathname{1,1} 'R00_vs_R00rms.png']);
close

end
```

Bibliography

[1] W.D. Myers and W.J. Światecki. Nucleus-nucleus proximity potential and superheavy nuclei. *Phys. Rev. C*, **62**:044610, Sep 2000.

[2] C.E. Aguiar, V.C. Barbosa, L.F. Canto, and R. Donangelo. Liquid-drop model description of heavy ion fusion at sub-barrier energies. *Nuclear Physics A*, **472**:571 – 590, 1987.

[3] W.J. Światecki. The dynamics of the fusion of two nuclei. *Nuclear Physics A*, **376**:275 – 291, 1982.

[4] K. Siwek-Wilczyńska and J. Wilczyński. Empirical nucleus-nucleus potential deduced from fusion excitation functions. *Phys. Rev. C*, **69**:024611, Feb 2004.

[5] J. Blocki, J. Randrup, W.J. Światecki, and C.F. Tsang. Proximity forces. *Annals of Physics*, **105**:427 – 462, 1977.

[6] Louis C. Vaz, John M. Alexander, and G.R. Satchler. Fusion barriers, empirical and theoretical: Evidence for dynamic deformation in subbarrier fusion. *Physics Reports*, **69**:373 – 399, 1981.

[7] I. Dutt. The role of various parameters used in proximity potential in heavy-ion fusion reactions: New extension. *Pramana*, **76**:921–931, 2011.

[8] W.D. Myers and W.J. Światecki. Nuclear masses and deformations. *Nuclear Physics*, **81**:1 – 60, 1966.

[9] K. Bethge, G. Walter, and B. Wiedemann. *Kernphysik: Eine Einführung*. Springer-Lehrbuch. Springer London, Limited, 2007.

[10] I. Angeli. A consistent set of nuclear rms charge radii: properties of the radius surface r(n,z). *Atomic Data and Nuclear Data Tables*, **87**:185 – 206, 2004.

[11] R.W. Hasse and W.D. Myers. Geometrical relationships of macroscopic nuclear physics. 1988.

[12] B. Nerlo-Pomorska and K. Pomorski. Simple formula for nuclear charge radius. *Zeitschrift für Physik A Hadrons and Nuclei*, **348**:169–172, 1994.

[13] W.D. Myers and W.J. Światecki. Nuclear properties according to the thomas-fermi model. *Nuclear Physics A*, **601**:141 – 167, 1996.

[14] M. Warda, X. Viñas, X. Roca-Maza, and M. Centelles. Neutron skin thickness in the droplet model with surface width dependence: Indications of softness of the nuclear symmetry energy. *Phys. Rev. C*, **80**, Aug 2009.

[15] B. Povh, K. Rith, C. Scholz, and F. Zetsche. *Teilchen und Kerne*. Springer-Lehrbuch. Springer-Verlag GmbH, 2004.

[16] Yi-Jin Shi and W.J. Swiatecki. Estimates of radioactive decay by the emission of nuclei heavier than α-particles. *Nuclear Physics A*, **438**:450 – 460, 1985.

[17] Liu Zu-Hua and Bao Jing-Dong. Effects of target deformation on the synthesis of superheavy nucleus ^{283} 112. *Chinese Physics Letters*, **21**(8):1491, 2004.

[18] W. J. Światecki, K. Siwek-Wilczyńska, and J. Wilczyński. Fusion by Diffusion. *Acta Physica Polonica B*, **34**:2049, 2003.

[19] H. A. Aljuwair, R. J. Ledoux, M. Beckerman, S. B. Gazes, J. Wiggins, E. R. Cosman, R. R. Betts, S. Saini, and Ole Hansen. Isotopic effects in the fusion of ^{40}Ca with ^{40,44,48}Ca. *Phys. Rev. C*, **30**:1223–1227, 1984.

[20] H. Timmers, L. Corradi, A.M. Stefanini, D. Ackermann, J.H. He, S. Beghini, G. Montagnoli, F. Scarlassara, G.F. Segato, and N. Rowley. Strong isotopic dependence of the fusion of 40ca + 90,96zr. *Physics Letters B*, **399**:35 – 39, 1997.

[21] J. D. Bierman, P. Chan, J. F. Liang, M. P. Kelly, A. A. Sonzogni, and R. Vandenbosch. Fusion barrier distributions for heavy ion systems involving prolate and oblate target nuclei. *Phys. Rev. C*, **54**:3068–3075, 1996.

[22] W. Reisdorf, F.P. Hessberger, K.D. Hildenbrand, S. Hofmann, G. Münzenberg, K.-H. Schmidt, J.H.R. Schneider, W.F.W. Schneider, K. Sümmerer, G. Wirth, J.V. Kratz, and K. Schlitt. Fusion near the threshold: A comparative study of the systems 40ar + 112, 116, 122sn and 40ar + 144, 148, 154sm. *Nuclear Physics A*, **438**:212 – 252, 1985.

[23] P.A. Tipler, G. Mosca, and D. Pelte. *Physik: Für Wissenschaftler und Ingenieure*. Sav Physik/Astronomie. Spektrum Akad. Verlag, 2004.

Curriculum Vitae

Personal

Name:	Manuela Gober, Bakk. rer. nat.
Nationality:	Austria

Education

9/1992 - 6/1996	Primary School (VS Strem, Burgenland)
9/1996 - 6/2000	Middle School (HS Güssing, Burgenland)
9/2000 - 6/2004	High School (BORG Güssing, Burgenland)
6/2004	A-Levels (Matura)
6/2005	Certificate in Advanced English
10/2005 - 7/2011	Bachelor Studies in Astronomy at the University of Vienna
Since 10/2006	Diploma Studies in Physics at the University of Vienna
Since 10/20011	Master Studies in Astronomy at the University of Vienna